Physics – Uspekhi **47** (3) 289 – 308 (2004)

METHODOLOGICAL NOTES PACS numbers: 03.65.Vf, 42.81.Gs, 42.87.Bg

Geometric phases in singlemode fiber lightguides and fiber ring interferometers

G B Malykin, V I Pozdnyakova

DOI: 10.1070/PU2004v047n03ABEH001722

Contents

Abstract. We consider various geometric phases (GPs) in singlemode fiber lightguides (SMFs) and in fiber ring interferometers (FRIs): the Pancharatnam phase stemming from the cyclic evolution of the polarization state of radiation (RP state) in SMF, the Rytov – Vladimirskiĭ phase (RV phase) stemming from the Rytov effect (specifically, rotation of the polarization plane due to noncoplanar winding of SMFs), as well as the nonreciprocal phase difference of counterpropagating waves (NPDCW) and nonreciprocal geometric phase of counterpropagating waves (NGPCW), which are caused by polarization nonreciprocity (PN) in FRIs. We show that in the general case, the Pancharatnam phase for an arbitrary RP state is inconsistent with the real phase change of light fluctuations in media that possess not only circular but also linear birefringence. We show that the RV phase, having a geometric origin, can in principle be considered as a dynamic phase (DP). We also show that the NGPCW can be considered as an effect of the evolution of the RP state mapped on the Poincaré sphere in Ginzburg's orthogonal screw polarization modes (GSPMs) of SMFs in the FRI contour. We analyze a number of experiments in which geometric phases were detected in FRIs: changing the RV phase and Rytov's angle (RA) in response to change of the pitch of helicoidal winding of SMFs.

G B Malykin Institute of Applied Physics, Russian Academy of Sciences, ul. Ul'yanova 46, 603950 Nizhniĭ Novgorod, GSP-120, Russian Federation
Tel. (7-8312) 16 48 70
E-mail: malykin@mail.nnov.ru; malykin@ufp.appl.sci-nnov.ru
V I Pozdnyakova Institute for Physics of Microstructures, Russian Academy of Sciences, 603950 Nizhniĭ Novgorod, GSP-105, Russian Federation
Tel. (7-8312) 67 57 32
E-mail: vera@ipm.sci-nnov.ru

Received 30 July 2003, revised 13 October 2003
Uspekhi Fizicheskikh Nauk **174** (3) 303 – 322 (2004)
Translated by V I Kisin; edited by A M Semikhatov

1. Introduction

In his well-known paper of twenty years ago [1], M Berry analyzed the conditions for the creation (existence) of a geometric (topological) phase that describes the evolution of the Schrödinger wave function in a system with a time-dependent Hamiltonian. This geometric phase (GP) is known as *Berry's phase*. Presently, the term 'Berry's phase' is often used not only in quantum mechanics but also in other fields (see reviews [2 – 7]). It must be mentioned that the main manifestations of the geometric phase in polarization optics were discussed in detail in the 1930s – 1950s by S M Rytov [8, 9], V V Vladimirskiĭ [10], and S Pancharatnam [11, 12] and even earlier in classical mechanics: 150 years ago by W R Hamilton [13] and 50 years ago by A Yu Ishlinskiĭ [14, 15] (see review [7]).

The present paper discusses various manifestations of geometric phases in singlemode fiber lightguides (SMFs) and in fiber ring interferometers (FRIs). FRIs are mostly used as fiber-optics gyroscopes (FOGs) — sensors of angular velocity [16]. The principle of the functioning of the FOG is based on the Sagnac effect [17 – 21] that produces a phase difference between counterpropagating waves in the FRI. Furthermore, FRIs have other uses — both fundamental and purely application-oriented — discussed in detail in review [16].

There are several reasons why we decided to discuss the geometric phases in FRIs. First, the geometric phase in the Michelson and Mach – Zender interferometers has already been analyzed in sufficient detail and there exists a large number of experimental and theoretical publications devoted to this aspect (see review [2]). Second, counterpropagating waves in FRI travel over equal optical paths and the phase difference can originate exclusively in nonreciprocity effects (e.g., Sagnac, Fiseau, and Faraday effects), and therefore the phase difference caused by length inequality between interferometer arms can be excluded from consideration (because it has no bearing on the geometric phase aspects). Third, in contrast to fiber interferometers of other types, a remarkable topological (geometric) phenomenon occurs in FRIs — the so-called polarization nonreciprocity (PN) [16, 22, 23], which leads to a nonreciprocal phase difference of counterpropagating waves (NPDCWs), also known as the zero shift in FRIs. If the radiation source used in an FRI is nonmonochromatic, the interference of counterpropagating waves that travel through the slow and fast birefringence axes of SMF can be treated separately, and the concept of nonreciprocal geometric phase of counterpropagating waves (NGPCWs) can be introduced for each of the independent interference patterns [24]; the NGPCW can be defined on the Poincaré sphere. The main difference between the NPDCW and NGPCW on the one hand, and the Rytov – Vladimirskiĭ phase (RV phase) and the Pancharatnam phase on the other hand is that the former remain nonreciprocal despite the fact that they are generated in a reciprocal medium. Therefore, three different types of geometric phases can exist simultaneously in FRIs.

The Pancharatnam phase (PP) and the Rytov – Vladimirskiĭ phase were previously considered in the framework of the so-called helical photons [2] having circular polarization [25]. However, an arbitrary radiation polarization state (RP state) can occur in SMFs. It is shown below that the concepts of PP and RV phases can be extended to an arbitrary RP state only if both orthogonal polarization modes in SMFs are excited with equal weights. In particular, it is shown in what follows that in the general case, the value of the Pancharatnam phase does not always coincide with the actual change of the phase of light oscillations — not only in optically active media (this was known previously [2]) but also in linearly birefringent media. Later in the paper, we point to a simple and visually clear physical interpretation of the Rytov effect and show that the term 'Pancharatnam phase' covers two different geometric phases with very distinct physical meanings.

The physical meaning of the Pancharatnam phase and a number of its characteristic features were treated in Refs [22, 23] (see also Section 5.3 of review [16]); however, these results need further elaboration concerning FRIs with an imperfect (nonideal) polarizer; this is done in Section 6.

We also discuss experimental observations of the geometric phase in FRIs [26 – 28]. These results were discussed in [16, 29] but the matter requires additional analysis, which we give in Section 7.

2. Review of the literature. Emergence of the concepts of geometric phases in polarization optics and fiber ring interferometry

We begin with the Rytov effect. S M Rytov has shown [8, 9] that when a linearly polarized light beam propagates along a nonplanar trajectory, the beam polarization plane rotates relative to the natural Frenet trihedron, formed by the tangent, the normal, and the binormal unit vectors, that accompanies the beam. This is what we mean by the Rytov effect. V V Vladimirskiĭ soon showed that the angle of rotation of the light polarization plane with respect to the initial angle measured from the normal is numerically equal to the area of the figure on the unit-radius sphere bounded by a closed curve drawn on this sphere by the tangent to the beam trajectory in the process of spatial evolution of the Frenet trihedron [10]. Neither Rytov nor Vladimirskiĭ wrote anything about the phase corresponding to the Rytov effect. To the extent of our knowledge, it was first mentioned in Ref. [30] that the rotation of the polarization angle caused by the beam propagation along a nonplanar trajectory corresponds to a certain phase increment. It was suggested that one refer to the phase acquired by a circular photon (or a beam with a circular RP state) in a lightguide with nonplanar winding as the Rytov – Vladimirskiĭ (RV) phase. The RV phase is a formal consequence of the fact that the lightguide acquires circular birefringence owing to the nonplanar winding.

Rytov's papers [8, 9] were published in 1938 – 1940, and that of Vladimirskiĭ [10] in 1941 in *Dokl. Akad. Nauk SSSR* (*Soviet Physics Doklady*). Because this journal was not translated into English at the time, these publications were mostly unknown outside the USSR (see, e.g., Refs [31, 32]). We note that the Rytov effect was multiply 'rediscovered' (see, e.g., Refs [30, 33 – 40]), by M Berry himself [39], among others.

In 1956, S Pancharatnam (Bangalore, India) considered not one but, in fact, two different geometric phases [11, 12]. Later, different authors applied the same term, 'Pancharatnam phase,' to different types of geometric phases, creating additional misunderstandings in some cases. Only in review [2] were we able to find a simultaneous description of both Pancharatnam geometric phases, but even there the two are given the same name. Pancharatnam first considered the phase difference between two completely polarized beams in different RP states, with no optical (conventional) phase difference [11], and showed that it can be defined on the Poincaré sphere [41, 42]. Pancharatnam also showed [11] that if the RP state of one of the beams varied cyclically (i.e., returned to the initial state), its phase (with the optical phase corresponding to a given evolution subtracted) would not equal the initial phase.

In what follows, we specifically refer to the Pancharatnam phase caused by the difference between the radiation polarization states of two interfering beams as the Pancharatnam phase 1 (PP1), and to that caused by the cyclic evolution of the radiation polarization state of one beam as the Pancharatnam phase 2 (PP2). The phase mostly discussed in the literature is PP2. Papers [11, 12] published in the Proceedings of the Academy of Sciences of India went practically unnoticed at the time of publication.

S M Rytov's [8, 9], V V Vladimirskiĭ's [10], and S Pancharatnam's [11, 12] results became widely known at the end of the 1980s and the beginning of the 1990s when Berry's work [1] stimulated considerable interest in geometric phases. For instance, papers [8, 10] were included in collected papers [43], and paper [11] in Ref. [44]. It must also be mentioned that M Berry contributed significantly to making the work of Pancharatnam, Rytov, and Vladimirskiĭ widely known. In Ref. [45], he described Pancharatnam's work [11] and in Ref. [46], wrote about the work of Rytov [8] and Vladimirskiĭ [10].

The history of the discovery of the nonreciprocal phase difference of counterpropagating waves and the nonreciprocal geometric phase of counterpropagating waves is closely related to the study of fiber ring interferometers and the discussion and further investigation of polarization nonreciprocity. Immediately after the development of the fiber ring interferometry in 1976 [47], it was discovered that a fairly large phase shift of the interference pattern of two counterpropagating waves occurs at the interferometer output; this so-called zero shift is not connected with rotation [48]. The cause of this phenomenon is the polarization nonreciprocity of the FRI contour; however, this effect was unknown at the time, not only to experts in fiber gyroscopes, but even to those who worked in polarization optics.

The phenomenon was explained independently and practically simultaneously by V N Logozinskiĭ [49] (Moscow), R Ulrich and M Johnson (Stuttgart, FRG) [50], and G Schiffner and colleagues (Munich, FRG and Vienna, Austria) [51]. These authors showed that polarization nonreciprocity stems from the difference between excitation conditions for counterpropagating waves at the entrance to an FRI and results in a nonreciprocal phase difference of the counterpropagating waves at the output of the FRI. It appears that Schiffner was the first to understand this; in January 1978, he submitted a German patent [52] that proposed to eliminate polarization nonreciprocity in FRI by installing two identical linear polarizers with identical orientation of transmission axes in each of the inputs of the FRI contour. Schiffner was obviously in no hurry to publish his results in the open press. In mid-January 1979, he submitted two similar and simultaneous patent applications [52] and then very similar applications for US patents [53, 54], and only by the end of January submitted a paper to *Applied Optics* [51], which was published in July of the same year. However, two months before, in May 1979, information about polarization nonreciprocity and a method of eliminating it was publicly discussed at the presentation of the diploma project of a student of the Moscow Institute for Physics and Technology, V N Logozinskiĭ [49], supervised by a well-known expert in laser gyroscopes, S A Gordon (see also [55]). At about the same time, Ulrich and Johnson published their paper [50].

It must be noted that the method of eliminating polarization nonreciprocity in FRIs suggested by Schiffner [51–54] proved rather unsuccessful because it required the use of two expensive polarizers within the fiber ring interferometer, and most importantly, they needed very precise mutual adjustment.[1] In 1980, Ulrich proposed the so-called minimal FRI contour [56] (Fig. 1), which has considerable advantages over earlier proposals [49–55] in that the contour includes only one polarizer placed within the FRI contour between two beam splitters. This FRI design gained the widest popularity.

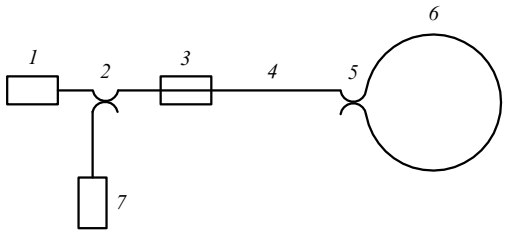

Figure 1. FRI schematic diagram: *1* — superluminescent diode, *2*, *5* — beam splitters, *3* — polarizer, *4* — SMF segment between the polarizer and the second beam splitter, *6* — FRI contour, *7* — photodiode.

A considerable number of papers were later devoted to polarization nonreciprocity in fiber ring interferometers (see, e.g., Refs [57–95]), but none of them explained the physical meaning of the polarization nonreciprocity phenomenon, and the nonreciprocal phase difference of counterpropagating waves caused by polarization nonreciprocity was not treated as a manifestation of geometric phases. In 1996, one of the authors of this review showed [24] that NPDCWs can be reduced to a geometric phase (NGPCWs) because the NPDCW, calculated separately for counterpropagating waves arriving along the slow and fast axes of the singlemode fiber waveguide in the FRI contour, is numerically equal to half the area of the spherical triangle on the Poincaré sphere formed by points corresponding to the state of radiation polarization at the input and both outputs of the contour. The Poincaré sphere method proposed in Ref. [24] proved convenient in a number of cases of polarization nonreciprocity. In the general case, the Poincaré sphere method [24] makes it possible to illustrate the polarization nonreciprocity phenomenon in FRI quite clearly and helps to understand it in clearer terms.

The polarization nonreciprocity phenomenon was analyzed in Refs [22, 23] (see also Section 5.3 of review [16]). For instance, it was shown in these papers that the polarization nonreciprocity phenomenon occurs even in FRIs containing a singlemode fiber waveguide with only one polarization mode,[2] and that the creation of polarization nonreciprocity occurs because the FRI contour is not equivalent to a straight or curved segment of the singlemode fiber lightguide: it is a nonconventional loop of the lightguide whose end segments are parallel to one another (see Fig. 1). As a result, the reciprocity conditions lead to different requirements for the structure of the Jones matrices [41] that describe the singlemode fiber lightguide and those that describe the FRI contour: the nondiagonal elements of the Jones matrix of the SMF segment must be equal in magnitude and have opposite signs, while for an FRI contour, the nondiagonal elements of the Jones matrix must be equal. However, papers [22, 23] contain the statement that "...the effects of polarization nonreciprocity are in a way 'virtual' or 'hidden' because additional phase difference must be present if we want to detect them" [16].[3] This statement is valid only for FRIs without a polarizer or with an ideal polarizer.

[1] A similar technique was proposed in Ref. [49]; in Ref. [50], it was suggested that one polarizer be installed after the radiation source and the other in front of the radiation receiver.

[2] An erroneous statement was often quoted in the past, namely, that the FRI polarization nonreciprocity is due entirely to the presence of two channels, that is, of two interfering orthogonal polarization modes.

[3] The phase difference meant here was caused by the 'true' nonreciprocal effects (Faraday, Fiseau, Sagnac) or by a mismatch of wavefronts of counterpropagating waves, etc.

In what follows, the main relations for geometric phases in singlemode fiber lightguides and in fiber ring interferometers, as well as the physical interpretations, are discussed in detail.

3. Pancharatnam phases

3.1 Poincaré sphere techniques

Because the Pancharatnam phases are defined on the Poincaré sphere, we begin with a brief exposition of the method of describing light polarization on the Poincaré sphere [41, 42] (Fig. 2). It is common knowledge that there exists a one-to-one correspondence between points on the Poincaré sphere and all possible radiation polarization states. Thus, points located on the 'equator' correspond to the linear polarization with various azimuths, the 'north pole' N corresponds to the right-circular polarization, and the 'south pole' S corresponds to the left-circular polarization. Points lying on the same 'meridian' correspond to the radiation polarization state with equal azimuths of the larger axis of the ellipse and different ellipticities (the closer to the pole, the greater the ellipticity). Points lying at the same 'latitude' correspond to RP states with equal ellipticities and different azimuths of the greater axis of the ellipse. Mutually orthogonal RP states (which are elliptic in the general case, with opposite directions of path tracing and with orthogonally oriented larger ellipse axes) correspond to diametrically opposite points on the Poincaré sphere. We remind the reader that angles in real space are doubled on the Poincaré sphere.

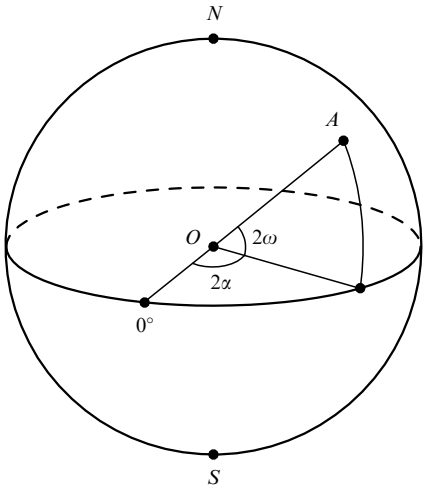

Figure 2. The Poincaré sphere: 2α — latitude of point A, 2ω — longitude of point A, point N — 'north pole', point S — 'south pole'.

3.2 Pancharatnam phase of the first kind

Pancharatnam first considered the phase difference arising between two beams with intensities I_1 and I_2 that have unequal RP states but zero conventional phase difference [11]. The polarization states of these beams correspond to points A and B on the Poincaré sphere (Fig. 3). The state of polarization of the sum (interference) of two beams corresponds to point C, and the intensity of the sum of two beams is described by the expression

$$I = I_1 + I_2 + 2\sqrt{I_1 I_2}\,\cos\frac{c}{2}\cos\delta\,, \qquad (1)$$

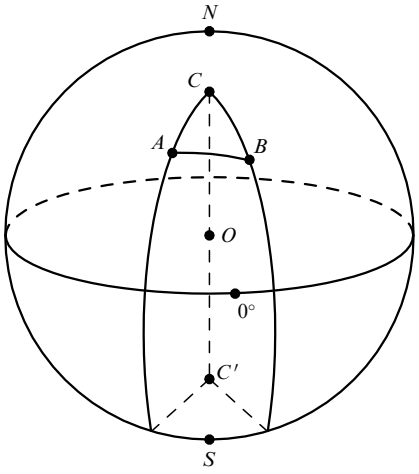

Figure 3. Pancharatnam phase of the first kind (PP1) mapped on the Poincaré sphere. Points A and B correspond to the polarizations of the two beams, point C is the polarization of their sum, and point C' maps the polarization orthogonal to that given by C.

where the angle c equals the arc AB (an arc on a sphere is always a segment of a circumference of the sphere); the quantity $\cos(c/2)$ determines the visibility of the interference pattern;[4] δ is the effective phase difference between two beams due to the difference between their polarizations, that is, the Pancharatnam phase of the first kind (PP1),

$$\delta = \pi - \frac{1}{2}\,\Theta_{ABC'}\,,$$

where $\Theta_{ABC'}$ is the solid angle, with apex at the center of the Poincaré sphere (point O), that subtends this spherical triangle ABC'; and C' is the point on the Poincaré sphere diametrically opposite to C. Because δ is measured in radians, and $\Theta_{ABC'}$ in steradians, we mean numerical equality. If the radius of the Poincaré sphere equals unity, the angle $\Theta_{ABC'}$ is numerically equal to the area of the triangle $S_{ABC'}$. We note that the quantity δ can be calculated using the Jones matrix techniques [41].

In Ref. [11], Pancharatnam analyzed the interference of totally coherent beams and in Ref. [12], of partially coherent beams.

3.3 Pancharatnam phase of the second kind

The Pancharatnam phase of the second kind (PP2) is a much more complicated subject. It can be defined unambiguously only for the cyclic evolution of an RP state, but even then it does not always correspond to the actual phase change of light oscillations. Pancharatnam himself did not conduct any specific analysis of how the cyclic evolution of an RP state occurs, that is, what the anisotropic elements are through which a light beam passes in the process. Even though a large number of theoretical and experimental papers were devoted to this problem (relevant references can be found in the bibliography of review [2]), it is not established in the general case under what conditions the actual change in the phase of light oscillations corresponds to PP2. The only discussion of this problem is given in [2] but in only one particular case of

[4] If the polarizations of the beams are orthogonal, the points A and B on the Poincaré sphere are diametrically opposite, $c = \pi$, and therefore $\cos(c/2) = 0$; hence, the visibility is also zero.

optically active media. In what follows, we discuss this problem in the general case.

As we mentioned earlier, PP2 was considered for the so-called helical (circular) photons [2], which correspond to a field with a specific value of the spin operator (i.e., to the so-called 'pure' states), because the photon — a massless particle — can only have two values, ± 1, of the projection of the angular momentum (spin) on its velocity direction [25]. But calculations of geometric phases in polarization optics must be carried out for arbitrary RP states.

In order to better understand the physical meaning of PP2 and the methods of its mathematical description, we consider three simple examples in which an RP state of an arbitrary type undergoes a cyclic evolution as the beam passes through various polarizers and circular and linear phase plates; we then calculate the value of PP2 in these cases using the Poincaré sphere technique and the Jones matrix technique [41]. For simplicity, we consider discrete optical elements, assuming among other things that polarizers have optical thickness so small in comparison with wavelength that the phase increment acquired in them is negligibly small. The medium between optical elements is assumed to be polarization-isotropic, and the phase increment acquired in it neglected, because it can always be subtracted.

Example 1. Let a monochromatic light beam with linear polarization and horizontal azimuth pass successively through a right-circular polarizer, then a linear polarizer whose transmission axis is at an angle α to the horizontal, and a linear polarizer with a horizontally oriented transmission axis, after which the RP state returns to the initial one (Fig. 4). Here, we assume all polarizers to be ideal in the sense that the polarization corresponding to the allowed direction is transmitted without loss, the orthogonal polarization is totally absorbed, and, furthermore, no additional phase increments are created. We also assume that $\alpha \neq \pi/2 \pm K\pi$, where K is an integer (otherwise the intensity at the output of the third polarizer is zero). Therefore, the initial RP state in Fig. 4 corresponds to point A that lies on the 'equator' and has zero longitude. After passing through the right-circular polarizer, light has right-circular polarization, which corresponds to point N, and having then passed through the first linear polarizer, light acquires linear polarization with azimuth α, which corresponds to point B on the equator of the Poincaré sphere with longitude 2α. Finally, light leaving the second polarizer again acquires linear horizontal polarization corresponding to point A. The solid angle on the Poincaré sphere subtended by the spherical triangle ANB equals 2α. Therefore, the value of PP2 equals α — half the solid angle 2α.

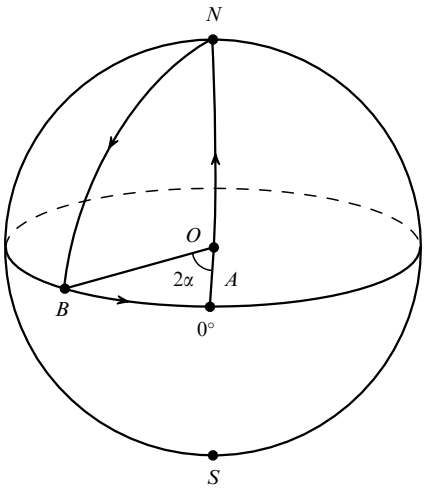

Figure 4. Mapping of the Pancharatnam phase of the second kind on the Poincaré sphere. Linearly polarized light passes consecutively through one circular and two linear polarizers. Point A corresponds to the initial and final radiation polarization states, and points N and B to intermediate RP states. Arrows indicate the direction of change of the RP state.

We now obtain the same result using the Jones matrix technique [41]. The relation between the Jones vectors at the entrance $\mathbf{E}_0$ and exit $\mathbf{E}$ of the system of the three polarizers discussed has the form

$$\mathbf{E} = \Pi_3 \cdot \Pi_2 \cdot \Pi_1 \cdot \mathbf{E}_0 , \tag{2}$$

where

$$\mathbf{E}_0 = \begin{pmatrix} 1 \\ 0 \end{pmatrix}$$

is the Jones vector of linearly polarized light with horizontally oriented azimuth,

$$\Pi_1 = \frac{1}{2}\begin{pmatrix} 1 & -\mathrm{i} \\ \mathrm{i} & 1 \end{pmatrix},$$

$$\Pi_2 = \begin{pmatrix} \cos^2\alpha & \sin\alpha\cos\alpha \\ \sin\alpha\cos\alpha & \sin^2\alpha \end{pmatrix},$$

$$\Pi_3 = \begin{pmatrix} 1 & 0 \\ 0 & 0 \end{pmatrix}$$

are the respective Jones matrices of the right-circular polarizer, of the linear polarizer with the transmission axis oriented at the angle α to the horizontal, and of the linear polarizer with the horizontal transmission axis. After simple calculations, we obtain

$$\mathbf{E} = \frac{1}{2}\begin{pmatrix} \cos^2\alpha + \mathrm{i}\sin\alpha\cos\alpha \\ 0 \end{pmatrix}$$

$$= \frac{\cos\alpha}{2}\begin{pmatrix} \cos\alpha + \mathrm{i}\sin\alpha \\ 0 \end{pmatrix} = \frac{\cos\alpha}{2}\begin{pmatrix} \exp(\mathrm{i}\alpha) \\ 0 \end{pmatrix}. \tag{3}$$

We have thus established again that the phase increment due to RP state evolution equals α and, therefore, the value of PP2 calculated using the Poincaré sphere techniques and the phase increment calculated using the Jones matrix techniques equal one another.

Example 2. Let a monochromatic light beam that in the general case has elliptic polarization and horizontal azimuth pass through a right-circular phase plate (an optically active medium) that creates the phase difference $\delta = 2\pi$ between slow and fast axes, such that the larger and smaller axes of the polarization ellipse at the output of the plate rotate by π; therefore, as in the example discussed above, the RP state returns to the initial state (Fig. 5). In Fig. 5, the initial (and final) RP states correspond to point A on the Poincaré sphere, with the latitude 2ω and longitude $\alpha = 0$. A cyclic variation of the RP state then corresponds to the parallel on the Poincaré sphere with the latitude 2ω. The opening angle of the cone with apex at the center of the Poincaré sphere and the base coinciding with the parallel at latitude 2ω is 2Θ, where

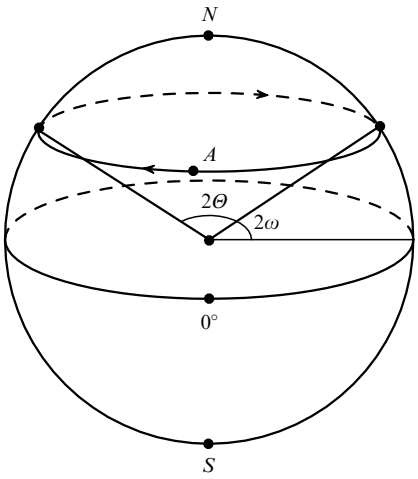

Figure 5. Mapping of the Pancharatnam phase of the second kind (PP2) on the Poincaré sphere. Elliptically polarized light passes through an optically active medium — circular phase plate with phase shift 2π. Point A corresponds to the initial and final RP states. The angle 2ω characterizes the ellipticity of the polarization of light. Arrows indicate the direction of change of the RP state.

$\Theta = \pi/2 - 2\omega$, and the solid angle χ at the apex of this cone is [96]

$$\chi = 4\pi \sin^2 \frac{\Theta}{2} = 2\pi(1 - \sin 2\omega)\,. \tag{4}$$

Therefore, the value of PP2 for a linearly polarized beam ($2\omega = 0$) is maximal and equals π (half the solid angle χ); PP2 is zero for right-circular polarization of the beam and falls in the interval $[0, \pi]$ for elliptic polarization.

We now use the Jones matrix technique to calculate the phase increment. The expression relating the Jones vectors at the entrance $\mathbf{E}_0$ and exit $\mathbf{E}$ has the form

$$\mathbf{E} = C \cdot \mathbf{E}_0\,, \tag{5}$$

where

$$\mathbf{E}_0 = \begin{pmatrix} \cos R \\ \mathrm{i} \sin R \end{pmatrix},$$

$$C = \begin{pmatrix} \cos\dfrac{\delta}{2} & \sin\dfrac{\delta}{2} \\ -\sin\dfrac{\delta}{2} & \cos\dfrac{\delta}{2} \end{pmatrix} = \begin{pmatrix} -1 & 0 \\ 0 & -1 \end{pmatrix}$$

are respectively the Jones vectors of elliptically polarized light with the horizontal larger axis of the ellipse ($R = 2\omega$) and the Jones matrix of the right-circular phase plate with the phase difference for the right- and left-circular polarization $\delta = 2\pi$. We can assume without losing generality that $0 \leqslant R \leqslant \pi/4$ because otherwise the position of the larger axis of the polarization ellipse would jump by $\pi/2$ as the parameter R passes through the value $\pi/4$. We note that the latitude 2ω on the Poincaré sphere is related to R by $2\omega = \arcsin(\sin 2R \sin\psi)$ [41], where ψ is the phase difference between the orthogonal components of the electric field. In the case in question, we have $\psi = \pi/2$ and therefore $R = \omega$. Hence, the parameter R characterizes the ellipticity of the polarization, $\tan R = b/a$, where a and b are the larger and smaller axes of the ellipse, respectively [41].

After simple calculations, we obtain

$$\mathbf{E} = -\begin{pmatrix} \cos R \\ \mathrm{i} \sin R \end{pmatrix}. \tag{6}$$

The minus sign at the vector in (6) indicates that both its components have acquired the phase shift π in the course of cyclic evolution, regardless of the ellipticity of the initial polarization. This contradicts the result obtained above by the Poincaré sphere technique, which showed that the value of PP2 depends on the ellipticity of light polarization. Expressions (5) and (6) coincide only for $R = 0$, that is, for the linear polarization of light. Therefore, a particular example of an optically active medium allowed us to show that in the general case, PP2 cannot adequately describe the phase increment acquired in the course of cyclic evolution of a polarization state.

Example 3. Let a monochromatic light beam with linear polarization and azimuth oriented at an angle α to the horizontal plane pass through a linear phase plate that creates the phase difference 2π between the slow and fast axes, with the slow axis being oriented horizontally (Fig. 6). Both orthogonal linear polarizations are excited in this phase plate, with different weights in general, and therefore, the RP state undergoes gradual modification in the course of light passing through the plate.[5] The initial (and final) RP states in Fig. 6 correspond to point A on the equator on the Poincaré sphere at the longitude 2α. The cyclic evolution of the RP state corresponds in this case to a circle on the Poincaré sphere with its center on the 'equator' at the longitude $\alpha = 0$. The opening angle of the cone with apex at the center of the Poincaré sphere and the base coinciding with this circle equals $2\Theta = 4\alpha$ and the solid angle of the apex of this cone [96] is

$$\chi = 4\pi \sin^2 \frac{\Theta}{2} = 4\pi \sin^2 \alpha\,. \tag{7}$$

Therefore, if $\alpha = 0$, that is, if the azimuth of linear light polarization at the entrance to the phase plate coincides with

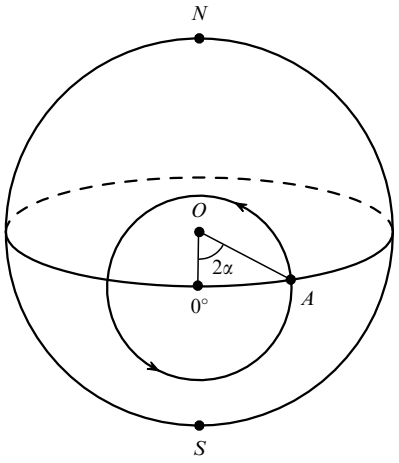

Figure 6. Representation of the Pancharatnam phase of the second kind (PP2) on the Poincaré sphere. Linearly polarized light passes through a linear phase plate with the phase shift 2π. Point A corresponds to the initial and final RP states. The angle 2α characterizes the azimuth of linear polarization. Arrows indicate the direction of change of the RP state.

[5] This variation of the RP state with time is known as *polarization beats*.

its slow axis, then $\chi = 0$ and PP2 is also zero. If $\alpha = \pi/4$, that is, if both linear polarizations in the slow and fast axes are excited with equal weight, then $\chi = 2\pi$ and PP2 is given by half the solid angle χ and is equal to π. If $\alpha = \pi/2$, that is, if the azimuth of the linear polarization of light at the entrance to the plate coincides with its fast axis, then $\chi = 4\pi$ and PP2 is correspondingly equal to 2π.

We now apply the Jones matrix technique to the calculation of the phase increment. The expression relating the Jones vectors at the entrance $\mathbf{E}_0$ and exit $\mathbf{E}$ of the phase plate is

$$\mathbf{E} = L \cdot \mathbf{E}_0 \,, \tag{8}$$

where

$$\mathbf{E}_0 = \begin{pmatrix} \cos\alpha \\ \sin\alpha \end{pmatrix},$$

$$L = \begin{pmatrix} \exp\left(\dfrac{i\delta}{2}\right) & 0 \\ 0 & \exp\left(-\dfrac{i\delta}{2}\right) \end{pmatrix} = \begin{pmatrix} -1 & 0 \\ 0 & -1 \end{pmatrix}$$

are respectively the Jones vector of linearly polarized light with azimuth oriented at an angle α to the horizontal and the Jones matrix of a linear phase plate with the phase difference $\delta = 2\pi$ for the slow and fast axes (for horizontal and vertical linear polarization). We then have

$$\mathbf{E} = -\begin{pmatrix} \cos\alpha \\ \sin\alpha \end{pmatrix}. \tag{9}$$

As in the previous case, the minus sign at the vector in Eqn (9) signifies that both its components acquired the phase shift by π. We see that in the case of a linear phase plate, PP2 coincides with the phase calculated using the Jones matrix technique only if $\alpha = \pi/4$.

A conclusion that can be made on the basis of the above analysis of cyclic evolution of the RP state in circular and linear phase plates is that PP2 may not correspond to the actual phase calculated by the Jones matrix technique if orthogonal polarizations are excited with unequal weights. On the other hand, if the RP state is such that only one of the orthogonal polarizations is excited in the phase plate (this RP state is known as an eigenstate for a given phase plate), then a dynamic phase is generated. A change in the dynamic phase does not correspond to a change in the RP state: the PR state does not vary in the course of propagation of the polarization eigenmode through an anisotropic medium, and the point representing it on the Poincaré sphere remains stationary, whereas the dynamic phase changes by the quantity $\pm\pi\Delta n z/\lambda$ (where Δn is the difference between refractive indices for the slow and fast axes of the phase plate and λ denotes the light wavelength in the vacuum) as a consequence of the difference between the refractive index for a given axis $n \pm \Delta n$ (the plus sign for the slow axis and the minus sign for the fast axis) and its average value n. Obviously, these constraints on PP2 also hold for a broad class of elliptic phase plates.

If the two polarization eigenmodes are excited with two different weights, it is impossible in general to separate PP2 and the dynamic phase [2]. An attempt to represent the real phase increment as a sum of PP2 and the dynamic phase was made [97], but it cannot be considered satisfactory: according to the definition in Ref. [97], the dynamic phase in the case of the cyclic evolution of the RP state is identically zero.

In the general case, therefore, PP2 for the cyclic evolution of polarization is only equal to the actual phase change (its measurement is conducted by the method of interference of the investigated beam and the reference beam whose phase and radiation polarization states are known) in the case where light travels through various combinations of polarizers of arbitrary types. The situation is more complex for phase plates: we were able to demonstrate in a number of particular cases that if two orthogonal polarizations are excited with different weights, then PP2 cannot be equal to the actual phase change.

We now consider the question, important in fiber ring interferometry, of the reciprocity of the Pancharatnam phases. Of course, PP1 cannot in principle be either reciprocal or nonreciprocal: it is merely an additional phase difference between two beams, caused by the difference between their polarizations. As for PP2, its reciprocity depends on the type of birefringence of the optical medium in which the cyclic evolution of the RP state unfolds. If this is conventional, circular, or linear birefringence, then PP2 is reciprocal. If, however, this circular birefringence is caused by the Faraday effect and the linear birefringence is caused by the electromagnetic nonreciprocal optical birefringence arising in crossed electric and magnetic fields [98 – 100], then PP2 is also nonreciprocal because the nonreciprocal increment $\pm\Delta n$ to the refractive index n has different signs for counterpropagating waves. If the phase increment is calculated by the Jones matrix technique, then the question does not arise because the sign of the phase for counterpropagating waves is taken into account automatically.

The main conclusion of this section is that in the most general case, it is advisable to calculate both the phase difference between two interfering beams with different polarizations and the additional phase difference created in the course of RP evolution using the Jones matrix technique or the equivalent method of expanding the field in geometric-optics (normal) waves [101 – 103]. We note that normal waves are plane waves, and polarization modes in singlemode fiber lightguides have a near-Gaussian transverse intensity distribution. But because the transverse distribution of light intensity is in most cases ignored (for instance, when the RP state and its phase in an SMF are calculated by the Jones matrix technique), normal waves in the SMF context are in fact mutually orthogonal polarization modes, which are typically elliptic.

Before we consider the Rytov effect and the Rytov – Vladimirskiĭ phases in fiber ring interferometers, it is necessarily to consider how the birefringence of an SMF is affected by bending and twisting of the optical guide as it is wound onto the spool of a fiber ring interferometer.

4. SMF birefringence due to its mechanical deformations

4.1 Kinematic phase in SMFs

First, we consider the phase increment in isotropic lightguides. As mentioned above, polarization in isotropic lightguides always acquires a phase increment $\varphi = 2\pi Ln/\lambda$ (the kinematic phase), which is proportional to the optical length of the waveguide Ln, where L is the lightguide length, n is the

effective index of the SMF, and λ is the wavelength of light in the vacuum. The kinematic phase is independent of the type of winding of the lightguide, provided the deformations caused by winding do not affect the value of n. Because counterpropagating waves travel over the same optical path in the FRI contour, kinematic phases of the counter propagating waves are equal even if the value of n is affected by the deformations caused by winding. Therefore, the kinematic phase cannot in any way change the result of interference of counterpropagating waves.

4.2 Linear birefringence of SMFs induced by bending

In the preceding section, we discussed the so-called isotropic singlemode fiber lightguide in which orthogonal polarization modes are degenerate. In a real SMF, however, some sort of polarization anisotropy is always present, and the effective refractive indices for orthogonal polarization modes slightly differ, covering the range from 10^{-3} for SMFs with strong linear birefringence to $10^{-9}-10^{-8}$ for the so-called coupled SMFs in which linear birefringence is largely suppressed. A nonplanar winding of a lightguide inevitably creates certain bending, which results in an additional linear birefringence β (rad m^{-1}) [104 – 106],

$$\beta = \frac{2\pi\rho}{\lambda}\left(\frac{d}{D}\right)^2, \tag{10}$$

where d is the lightguide diameter and D is the winding diameter; in quartz SMFs, $\rho = 0.133$. The birefringence β is related to the difference Δn between refractive indices for the slow and fast polarization modes of the SMF and to the light wavelength λ as $\beta = 2\pi\Delta n/\lambda$. From the standpoint of mathematical description in the plane-wave approximation, the fiber lightguide we consider does not differ in any way from a linear phase plate. The linear birefringence due to bending disturbs the inherent (nonperturbed) linear birefringence of the SMF (provided it is nonzero) and the two add up as vectors.

4.3 Circular birefringence in SMFs induced by twisting. Ginzburg's screw polarization modes

As a singlemode fiber lightguide is wound, the lightguide may in principle be twisted, causing torsional deformations and generation of the induced circular birefringence β_c, whose value is given by [104, 106 – 108]

$$\beta_c = 2(1-g)\,t,$$

where g is the photoelasticity coefficient, which is 0.065 – 0.080 for quartz SMFs [104, 106 – 108], and t is the fiber twisting per unit length (rad m^{-1}). If the lightguide has its proper (nonperturbed) linear birefringence, the polarization eigenmodes of a twisted SMF become elliptic [103, 109]. However, it is very inconvenient to describe a twisted SMF in the laboratory reference frame: the ellipticity and the azimuth of the larger axis of the ellipse of polarization eigenmodes of such an SMF, considered as integral characteristics of the entire segment of the SMF, are periodic functions of the lightguide length even if twisting is uniform.

This problem was solved in 1944 by V L Ginzburg [101] (see also Ref. [102]): he introduced the concept of screw polarization modes, that is, modes in a reference frame corotating with twisting. In this case, the ellipticity of polarization modes becomes independent of the lightguide length, the elliptic birefringence equals[6] $\beta_e = (\beta^2 + \beta_c^2)^{1/2}$, and the azimuth of the larger axis of the ellipse rotates together with the screw reference frame. In calculations of signals at the output of an SMF segment, we need to take the rotation of the helical reference frame into account. Ginzburg also formulated the condition of applicability of geometric optics in the case where twisting is constant and there is no linear interaction between normal waves [101, 102]:

$$2t \ll \beta. \tag{11}$$

If this condition is satisfied, polarization eigenstates of the medium with nonperturbed linear birefringence and torsional twist are weakly elliptic, that is, nearly linear, and can be treated as screw polarization modes [101, 102]. Condition (11) can be written in a somewhat different form $\beta_c \ll \beta$, stating that the circular birefringence induced by twisting must be much lower than the linear birefringence of the medium. If no linear birefringence was initially present, twisting cannot produce any circular birefringence in the medium [101, 102].

Ginzburg also showed that there is another condition for the applicability of geometric optics: $2t\lambda \ll \beta_c\lambda \ll 1$; however, this condition is always satisfied in actual optical media [101, 102]. It states that the phase difference due to twisting-induced circular birefringence building up along the optical path equal to the light wavelength must be much less than 1 radian. The physical meaning of this last condition is that there is no back reflection of the light wave in a twisted medium with nonperturbed linear birefringence. In quartz SMFs, this condition is satisfied with a large safety margin (of at least three orders of magnitude) because torsion stresses begin to destroy the lightguide only at twists of about 150 – 200 turns m^{-1} [109].

In the case of variable twisting, the adiabaticity condition was formulated in Ref. [103]: ellipticity of normal waves must vary weakly over the length of polarization beats in the SMF, $L_b = \lambda/\Delta n$. If this condition is satisfied, then linear interaction in the propagation of normal waves can be neglected in the first approximation. We note that energy exchange between two normal waves can be characterized qualitatively by the so-called polarization conservation parameter — the h-parameter [110 – 114]. The h-parameter was applied earlier to describe the coupling of linear polarization modes in singlemode fiber waveguides. Recently, it proved possible to generalize the concept of the h-parameter to polarization modes with arbitrary ellipticity [109, 115]. Obviously, even if the above condition is satisfied, it is no longer possible to neglect the linear interaction of normal modes (polarization modes) if there are a large number of inhomogeneities over a considerable length of the optical medium (such as the SMF).[7]

Ginzburg's results [101], just like those of Rytov [8, 9] and Vladimirskiĭ [10], went unused for a long time. It was only in 1972 that E V Suvorov [116] applied the results of [101] to describe the propagation of electromagnetic waves through a plasma in the presence of a shear of force lines of a magnetic field. In 1983, when it became necessary to describe the linear interaction between polarization modes in SMFs, the results presented in [101] were used in the paper by V V Zheleznyakov, V V Kocharovskiĭ, and Vl V Kocharovskiĭ [103]. Later,

[6] Paper [101] treated a linear phase plate with torsion stresses.

[7] The condition that is violated in this case is $hL \ll 1$, where L is the length of the SMF.

Ginzburg's method was used to describe random coupling of polarization modes in SMFs in the presence of linear birefringence [109] and of regular and random twisting. In particular, it was shown in Ref. [109] that in the case of random twisting, the SMF is characterized by three h-parameters, not by a single one as in Refs [110 – 114].

Because the results of Ginzburg's work [101] provide a simple and visually clear description of the RP state evolution in media with linear birefringence and twisting and are important in polarization optics, it is only fair to refer to screw polarization modes introduced in Ref. [101] as Ginzburg's screw polarization modes (GSPMs). In principle, they are equivalent to the conventional method of Jones matrices in a linear base and may provide certain advantages in specific cases. For this, it is necessary to pass to the elliptic base corresponding to mutually orthogonal GSPMs [117]. With this base, the Jones matrix of an SMF segment with Ginzburg's screw polarization eigenmodes becomes diagonal, which considerably simplifies calculations.

A legitimate question arises here: why did the results in Refs [8 – 10, 101] lay dormant for so long? These results were far ahead of the contemporary level of polarization optics, which was mostly oriented toward the needs of crystallography. Even though the results obtained by H Poincaré [118], N Wiener [119] (coherence matrix, 1930), and R C Jones and H Hurwitz [120 – 122] (Jones matrices and equivalence theorems in polarization optics, 1941) were well-known, most authors, as noted in review [42], ignored the results of these papers and carried out calculations using very cumbersome obsolete techniques until the beginning of the 1960s, that is, until U Shurkliff's monograph appeared in print [41].

5. The Rytov effect and Rytov – Vladimirskiĭ phase in SMFs and FRIs in the case of noncoplanar winding

5.1 The Rytov effect in a singlemode fiber lightguide of FRIs

We return to discussing the fiber ring interferometer (FRI). Because the FRI contour consists of a large number of turns wound onto an SMF spool, the end of each turn is shifted relative to the beginning of this turn by a distance of at least one diameter of the lightguide fiber. In this case, the lightguide has a noncoplanar (nonplanar) winding and the Rytov effect — rotation of the light polarization plane — is generated in it [8, 9]. The Rytov effect not only rotates the polarization plane of the beam but also rotates the transverse structure of the beam whenever that structure exists. For instance, rotation of the speckle structure of light was experimentally observed in a multimode lightguide wound on a spool; this rotation was numerically equal to the solid angle described by the tangent to the lightguide.

The angle of rotation of the polarization plane due to the Rytov effect per one turn of the singlemode fiber lightguide wound on a cylindrical spool (which we suggest be referred to as the Rytov angle, or RA) is

$$\gamma = 2\pi\left(1 - \frac{h}{\sqrt{(\pi D)^2 + h^2}}\right) = 2\pi(1 - \cos\theta)\,, \qquad (12)$$

where D is the diameter of the cylinder, h is the winding pitch of the SMF, and θ is the angle between the lightguide axis and the generatrix of the cylindrical spool. The total Rytov angle is given by

$$\alpha_{\mathrm{Ryt}} = K\gamma\,, \qquad (13)$$

where K is the integer equal to the number of turns.

We consider two types of windings of an SMF onto the spool of the FRI contour.

(1) Let the winding of the lightguide on the cylindrical spool be performed such that the axes of the inherent linear birefringence retain their orientation from one turn to the next, as shown in Fig. 7a. We note that this condition is met automatically in the winding of the so-called ribbon singlemode waveguide [124 – 126], whose cross section is nearly rectangular in shape and the birefringence axes are perpendicular to the sides of the rectangle. In this case, the fiber undergoes torsional twisting. The twisting t of the fiber per unit length and the angle T of rotation of the axes of linear birefringence per one turn of the fiber are found from the expressions [2]

$$t = \frac{2\pi h}{(\pi D)^2 + h^2}\,, \qquad T = \frac{2\pi h}{\sqrt{(\pi D)^2 + h^2}} = 2\pi - \gamma\,. \qquad (14)$$

We see in this particular case that although the axes of linear birefringence in the SMF retain their orientation from turn to turn, the polarization eigenmodes of such an SMF become elliptic as a result of the twisting. If the SMF eigenmodes were elliptic, this sort of turn stacking would change the degree of their ellipticity.

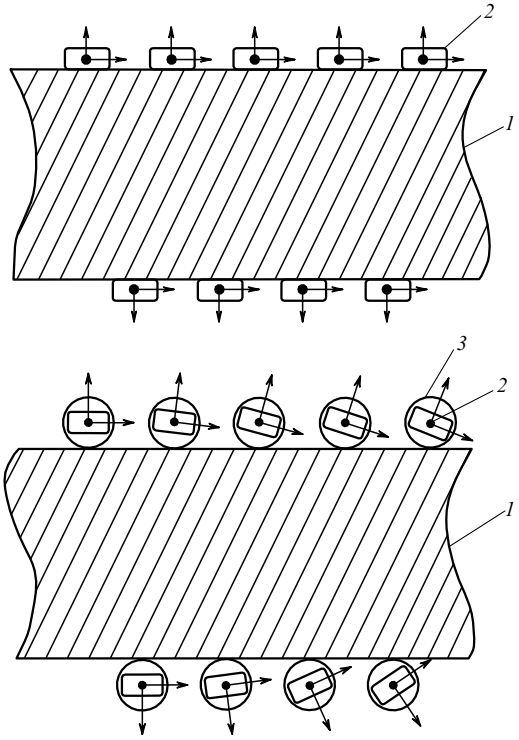

Figure 7. Transversal cross section of a spool with a ribbon singlemode fiber lightguide wound on it: (a) the lightguide is wound directly onto the spool; (b) the lightguide is inside a Teflon tube wound onto the spool: *1* — spool, *2* — ribbon singlemode fiber lightguide; *3* — Teflon tube. Arrows indicate directions of linear birefringence inside the SMF.

(2) A different type of SMF winding is used to measure the Rytov effect. In order to avoid torsional deformation of the lightguide in nonplanar winding, the lightguide is first placed in a Teflon tube with a low friction coefficient and is then wound onto a cylindrical spool [2, 26–28, 127–129]. The Teflon tube undergoes torsional deformation but the optical fiber does not — because the fiber readily unwinds inside the tube in such a way as to remove torsional strains. In this way, the structure of the SMF turns is not coplanar but the fiber is not twisted.

The orientation of linear birefringence axes in the transversal cross section of a ribbon SMF wound onto the spool in a Teflon tube is shown in Fig. 7b. The figure makes the physical meaning of the Rytov effect of the SMF with zero torsional twisting quite transparent: it consists in the rotation of the cross section and therefore of the linear birefringence axes in the lightguide from one turn to another as a result of the noncoplanar structure of the turns, that is, as a result of the geometric properties of the winding of the lightguide onto the spool.

Therefore, the Rytov effect is the rotation of the cross section and, correspondingly, of the SMF axes without any actual twisting of either the beam or the lightguide.

We note here that the value of the Rytov angle is independent of the presence or absence of torsional twisting of the fiber — these are two totally independent phenomena. Because the Rytov effect causes rotation of the polarization plane, it can be formally reduced to the emergence of some additional optical activity, that is, the emergence of an effective circular birefringence that in the laboratory reference frame is given by

$$\beta_c = 2\,t_{\text{eff}} = 2\,\frac{\gamma}{\sqrt{(\pi D)^2 + h^2}}\,, \qquad (15)$$

where t_{eff} is the effective fiber twisting per unit length due to the geometric properties of winding. In the helical reference frame [101, 103, 109] comoving with this twisting, the polarization eigenmodes within the SMF (Ginzburg's screw polarization modes) retain their ellipticity that was present before the lightguide was wound onto the spool. For example, if the inherent (nonperturbed) birefringence in the SMF was linear, then the GSPMs remain linearly polarized in the helical reference frame. This is not surprising because the Rytov effect is the emergence of rotation of the cross section and, correspondingly, of the axes of the SMF birefringence with zero twisting, that is, without generation of torsional strains; indeed, the optical activity caused by the Rytov angle is caused by the kinematic properties of the parallel translation of the Frenet trihedron along the beam trajectory or along the lightguide in the case of nonplanar winding, which is the same thing.

5.2 Similarities between the Rytov effect in polarization optics and the Ishlinskiĭ effect in classical mechanics. Parallel vector translation. Noncommutativity of finite rotations

As mentioned above, the Rytov effect is a manifestation of the so-called parallel translation, in this case, the translation of the Frenet trihedron along the lightguide that was wound in a nonplanar fashion. Such phenomena occur in various fields of physics and result in various topological phases, the difference between them being only that in some cases the translation occurs in real space (e.g., the Rytov effect) and in other cases in the parameter space. Parallel vector translation along a nonplanar surface is closely related to the so-called noncommutativity of finite rotations. A clear illustration of this phenomenon in mechanics is given in Fig. 8. A matchbox — a rectangular parallelepiped — successively undergoes three rotations by 90° around three different sides but is never rotated around its side with the striking surface (the one to the right of the label). But after three rotations, the matchbox is found to be rotated precisely around this side by 90°. If this matchbox rotation follows a different sequence, the rotation angle in the final position has the opposite sign relative to the initial position.[8] This is the reason why this phenomenon is known as *noncommutativity of finite rotations*. This effect, caused by the conical motion of a solid (referred to as 'coning' in the American literature) was already discussed by W R Hamilton [13] and later, in more detail, by A Yu Ishlinskiĭ [14, 15] (see also review [7]). Incidentally, as we showed in our publications [134, 135], this classic effect has a relativistic analog: the Thomas precession.

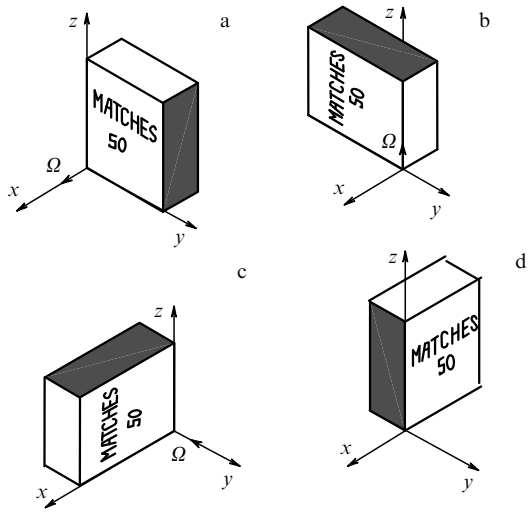

Figure 8. Geometric phase in classical mechanics: noncommutativity of finite rotations. A matchbox undergoes three successive rotations by 90° around different edges and as a result is rotated by 90° relative to the side around which is was not rotated: (a–d) the sequence of matchbox positions; Ω — matchbox rotation axis for each position.

We now consider the parallel translation operation as such. We imagine moving a matchbox along a spherical surface (e.g., along the surface of the earth) such that it always remains parallel to itself (Fig. 9). The matchbox first follows the equator, then goes up to the north pole along the meridian, then descends to the equator along another meridian 90° distant from the first, and finally returns to the initial point along the equator. If we ignore the translational motion, the matchbox performs the same operations as those shown in Fig. 8 and its rotation angle (90°) is numerically equal to the solid angle on the sphere subtended by the trajectory of the matchbox.

[8] S A Kharlamov demonstrated the rotation of a matchbox in the 1990s in his lectures on theoretical mechanics at the Mechanics and Mathematics Department of Moscow University [130] (see also the talk by N I Krobka [131]). This phenomenon was similarly illustrated by the case of a rotated book in volume I of the Berkeley Physics Course [132] and in the course of theoretical mechanics by V F Zhuravlev [133].

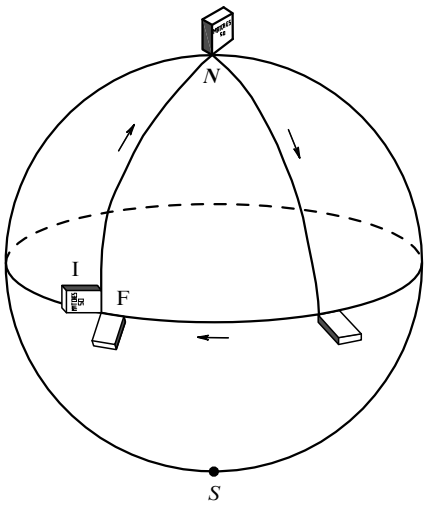

Figure 9. The geometric phase in classical mechanics: the parallel translation. A matchbox moves parallel to itself along a closed trajectory on the surface of the sphere, tracing a quadrant. As a result, having returned to the initial position, the matchbox has been rotated by 90°. I and F denote the initial and final positions of the matchbox.

The mechanical kinematic effect discussed above is directly analogous to the Rytov effect both from the standpoint of physical interpretation and from that of mathematical description. At the beginning of the 1950s, Ishlinskiĭ proved a theorem known as the *solid angle theorem* [14, 15], which was later reformulated by V F Zhuravlev as follows[9] [134, 136]: ''If a certain axis singled out in a solid with three degrees of freedom has spanned a closed conic surface in the process of motion of the body and the projection of angular velocity of the body on this axis was zero, then after the axis returns to the initial position, the body has rotated around this axis by the angle that is numerically equal to the solid angle of the spanned cone.'' Translational motion of the body does not affect the rotation angle. Ishlinskiĭ gave the following example to illustrate the situation [14, 15]. An axis with a frictionless flywheel mounted on it spans a solid angle; if the angular velocity of the flywheel (or rather its projection on the axis) is zero at the initial moment, then after the cyclic rotation of the axis has been completed, the flywheel has been rotated by the angle that is numerically equal to the solid angle spanned by the axis. We see that the rotation of the flywheel is connected with its inertial properties: to conserve its kinetic energy in translation, the flywheel must execute a rotation relative to the laboratory reference frame.

In view of this, we give another possible interpretation of the physical nature of the Rytov effect. As indicated in Kravtsov's monograph [32], ''...the Rytov equation reflects a certain inertia of field vectors that locally cannot follow the beam trajectory. These inertial properties are caused by the conservation of the field momentum.'' This interpretation agrees with Ishlinskiĭ's interpretation of the properties of parallel translations of the body in classical mechanics, also connected with the inertia of the body.

However, while the Rytov and Ishlinskii effects are completely analogous, in the general case there is no such analogy between the rotation angle acquired by a solid in the process of conic motion (the so-called Ishlinskiĭ angle) and the geometric phase in optics. A solid exists in conventional space, where we can always separate the displacement of a body, which is analogous to the kinematic phase in optics, from the angle of rotation of the body that can be related both to the conventional rotation in optics (analogous to the dynamic phase) and to its conic motion (analogous to the Rytov effect). Contrariwise, the kinematic and dynamic phases, the RV phase, the Rytov angle, and PP2 are generated in the process of light propagation through an optical medium, which is anisotropic in the general case. Rotations of a solid body related to its conic motion can be treated ignoring its displacements and rotation, but the changes in the kinematic phase, dynamic phase, RV phase, Rytov angle, and PP2 are inseparable from the translational motion of light in an optical medium, including SMF. Consequently, it is not always possible to separate the RV phase or PP2 from the dynamic phase.

In the presence of linear birefringence and irregular twisting, the evolution of the RV phase and the change in PP2 are described, even on a straight segment of an SMF, by more complicated differential equations than the conic rotation of a solid. Such an SMF is analogous, in the sense of mathematical description, to relatively complicated (so-called nonholonomic [139]) mechanical systems that can be exemplified with the gyrocompass discussed by Ishlinskiĭ [14, 15]; this gyrocompass consists of two coupled gyrocompasses. As shown in Refs [140–142], the evolution of the RP state and the change of PP2 in lightguides also occur in the presence of nonholonomic constraints.[10] Finding a useful mechanical analog of the RP state evolution is not a simple problem, but we were recently able to find a mechanical system that can be described by a set of differential equations similar to that describing an SMF with linear birefringence and irregular twisting [143].

5.3 The Rytov–Vladimirskiĭ phase and the Pancharatnam phase of the second kind in SMFs with noncoplanar winding

As shown above, the Rytov effect produces an equivalent optical activity in singlemode fiber lightguides (or changes it if it was already present in the SMF); hence, circularly polarized light propagating through a lightguide with noncoplanar winding acquires a dynamic phase, which has been suggested to be referred to as the Rytov–Vladimirskiĭ phase (RV phase) [2]. If light is already linearly polarized, a change is generated in the RP state, additional relative to the laboratory reference frame (indeed, birefringence does not change in the helical reference frame comoving with the special twisting, that is, Ginzburg's screw polarization modes preserve their ellipticity). In its turn, this change in the RP state causes an additional phase change, which is in fact the Pancharatnam phase of the second kind (PP2) for optically active media. As mentioned above, it is not always possible to separate the RP state and PP2 in the general case of the RP state.

We have shown above (see also [2]) that in optically active media, PP2 corresponds to the real phase change only when both circular polarization modes of the SMF are excited with equal weights, that is, when linearly polarized radiation is sent to the input of the SMF. Therefore, only in this particular case does the PP2 caused by the Rytov effect correspond to the real phase change of light oscillations.

[9] On the solid angle theorem, see also Refs [137, 138].

[10] We recall that one of the fundamental properties of nonholonomic systems is that they do not in general return to the initial state after a cyclic evolution [139].

Whether the RV phase is the geometric or dynamic phase is a matter of definition. The RV phase is a consequence of a purely geometric phenomenon (the Rytov effect causing optical activity of geometric origin) and is a geometric phase in this sense. But if the RV phase is treated as a consequence of optical activity, and the causes of this optical activity are not analyzed, it can be considered a dynamic phase.

If the SMF has no magnetic activity or has natural[11] optical activity simultaneously with linear birefringence, then the RV phase is reciprocal because the equivalent optical activity corresponding to the Rytov effect is also reciprocal. Otherwise, as shown in Ref. [103], the RV phase caused by the Rytov effect is nonreciprocal. It is obvious that in this case, the PP2 due to the Rytov effect is also nonreciprocal.

6. Polarization nonreciprocity in FRIs and the nonreciprocal geometric phase of counterpropagating waves

6.1 Polarization nonreciprocity in FRIs

As mentioned above, the polarization nonreciprocity effect arises in the FRI contour satisfying conventional reciprocity conditions [102] and is caused by the noncommutativity of anisotropic elements in the FRI contour and by their asymmetric orientation relative to the midpoint of the contour [16, 22, 23]. Specifics of manifestations of polarization nonreciprocity and its physical interpretation are discussed in detail in Refs [16, 22, 23, 144]. A number of particular cases of polarization nonreciprocity are discussed in Refs [57 – 95]. Here, we concentrate on discussing the polarization nonreciprocity and its effect on the nonreciprocal phase difference of counterpropagating waves (NPDCW) and on light intensity at the FRI output. The values of ellipticity of polarization modes in the SMF of the ring interferometer contour, the RP state at the FRI input, the extinction coefficient of the polarizer, and the orientation of birefringence axes of the SMF at the contour inputs are assumed to be arbitrary. This allow us to describe certain specific features, unknown earlier, of the polarization nonreciprocity effect in FRIs.

The formation of random coupling of polarization modes [109] on SMF inhomogeneities in an FRI contour greatly complicates the analysis of polarization nonreciprocity [66, 74, 80, 87, 89, 92, 94, 95] because the ellipticity and mode azimuths vary in a random manner (e.g., as the SMF temperature varies) and this in turn changes the zero shift of the FRI. In what follows, we consider fiber ring interferometers with SMF contours and regular birefringence, that is, without random inhomogeneities.

In the general case, natural polarization modes of SMF with regular birefringence are elliptic. We note that the effects connected with polarization nonreciprocity in FRIs whose contour is made of a singlemode fiber lightguide with linear birefringence are well known [16, 22, 23, 66, 74, 79], and in FRIs whose contour is made of SMFs with circular birefringence, the phase difference of counterpropagating waves due to polarization nonreciprocity is zero. This was proved by the Jones matrix technique in Ref. [84] and by the Poincaré sphere method in Ref. [24].

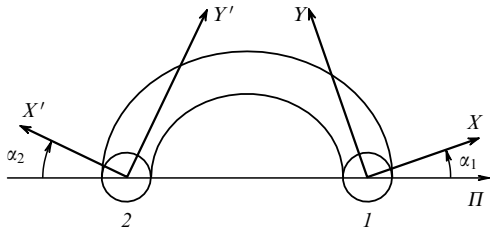

Figure 10. Orientation of axes of inherent linear birefringence at the input to the FRI contour: X, Y and X', Y' are the directions of the slow and fast axes, respectively, at the inputs *1* and *2* of the contour.

Two different factors exist that produce polarization nonreciprocity in FRIs with a single mode fiber lightguide contour having regular birefringence. In what follows, we use PN1 and PN2 to denote polarization nonreciprocity types caused by these two distinct factors.

(1) PN1 arises only if the birefringence axes of the SMF at different inputs of the FRI contour do not coincide. PN1 can be regarded as a consequence of nonsimultaneous excitation of the input radiation field of each polarization eigenmode at the two ends of the contour. This factor is independent of the coherence properties of radiation. The value of the NPDCW due to PN1 depends on the angle between the birefringence axis of the SMF at the inputs to the FRI contour, the RP state at the FRI input, and the ellipticity of the SMF polarization modes in the FRI contour. Because the NPDCW is related to the topological characteristics of the FRI fiber contour — its loop shape and rotation of the SMF axes at the contour input — the NPDCW can be considered a geometric phase.

(2) PN2 is caused by the two-channel nature of the process (the propagation of the radiation of counterpropagating waves in the FRI contour in two orthogonal polarization modes, or channels), by coherence or partial coherence of radiation in orthogonal modes after passing through the FRI contour, and the interference of polarization modes because of the noncoinciding axes of anisotropy in the single mode fiber at the input (output) of the fiber contour, or because the polarizer in the FRI circuit (Fig. 10) is not oriented parallel to one of the SMF axes. In this case, regardless of the RP state at the FRI input, the interference signal at the output can carry additional information on the phase difference of light waves that passed along the slow and fast birefringence axes in the SMF contour; this birefringence is directly proportional to the linear birefringence times the fiber length and may vary in response to mechanical factors acting on the SMF contour and in response to temperature changes that affect the FRI contour length L and the value of birefringence. Presently, FRIs use nonmonochromatic light sources and the condition[12] $L \gg l_{\mathrm{dep}}$ is always met and the counterpropagating waves passing along different birefringence axes of an SMF are not coherent relative to one another. In this case, the NPDCW is caused by PN2.

We note here that as shown in Refs [66 – 74] (see also Ref. [16]), polarization nonreciprocity is caused by the RP state of one type or another at the FRI input. If radiation at

[11] The natural optical activity stems from the susceptibility of the optical medium (e.g., water solution of sugar) to rotation of beam polarization. The circular birefringence of the medium, stemming from its torsional twisting, is not optical activity.

[12] l_{dep} is the depolarization length of nonmonochromatic radiation in SMFs ($l_{\mathrm{dep}} = \lambda_0^2/(\Delta\lambda\Delta n)$ [114], where $\Delta\lambda$ is the spectral width of the radiation source).

the FRI input is completely depolarized, there is no polarization nonreciprocity.

Figure 10, which shows the orientation of the inherent linear birefringence axes in the SMF at both inputs of the FRI contour, illustrates the fact that the radiation propagating along the axis X acquires an additional phase increment by π radians in comparison with the radiation propagating along the axis Y; in calculations later in this section, this is taken into account by introducing a half-wave phase plate.

We write the expressions for the electric fields of both counterpropagating light waves at the input and output of the FRI in the presence of rotation when a phase difference Φ_S due to the Sagnac effect appears in the FRI:

$$\Phi_S = \frac{8\pi N s \Omega}{\lambda c} . \tag{16}$$

Here, λ is the light wavelength in the vacuum, c is the speed of light in the vacuum, s is the area of the projection of one turn of the FRI fiber contour on the plane orthogonal to the angular velocity vector, N is the number of turns in the FRI contour, and Ω is the angular velocity of rotation.

The vectors of electric fields of counterpropagating waves at the FRI output,

$$\mathbf{E}^+ = \begin{pmatrix} E_x^+ \\ E_y^+ \end{pmatrix} \quad \text{и} \quad \mathbf{E}^- = \begin{pmatrix} E_x^- \\ E_y^- \end{pmatrix}$$

(in the Cartesian coordinates based on the allowed and forbidden axes of the linear polarizer[13]), are given by

$$\mathbf{E}^+ = \Pi \cdot \frac{\lambda}{2} \cdot T(-\alpha_2) \cdot K^+ \cdot T(\alpha_1) \cdot \Pi \cdot \mathbf{E}_0 \cdot \exp\left(\frac{i\Phi_S}{2}\right),$$

$$\mathbf{E}^- = \Pi \cdot T(-\alpha_1) \cdot K^- \cdot T(\alpha_2) \cdot \frac{\lambda}{2} \cdot \Pi \cdot \mathbf{E}_0 \cdot \exp\left(-\frac{i\Phi_S}{2}\right), \tag{17}$$

where

$$\mathbf{E}_0 = \begin{pmatrix} A_x \\ A_y \exp(i\psi) \end{pmatrix}$$

is the normalized Jones vector at the FRI input ($A_x^2 + A_y^2 = 1$) and

$$\Pi = \begin{pmatrix} 1 & 0 \\ 0 & \varepsilon \end{pmatrix}, \quad T(\alpha) = \begin{pmatrix} \cos\alpha & \sin\alpha \\ -\sin\alpha & \cos\alpha \end{pmatrix}, \quad \frac{\lambda}{2} = \begin{pmatrix} -1 & 0 \\ 0 & 1 \end{pmatrix}$$

are the respective Jones matrices of the linear polarizer, of the rotation of one of the ends of the contour by an angle α, and of the half-wave plate. The matrices K^+ and K^- describe the FRI contour depending on the direction of path tracing; $K^- = (K^+)^T$ and

$$K^+ = \begin{pmatrix} \cos\frac{\delta}{2} + i\sin\frac{\delta}{2}\cos 2R & \frac{1}{2}\sin\frac{\delta}{2}\sin 2R \\ -\frac{1}{2}\sin\frac{\delta}{2}\sin 2R & \cos\frac{\delta}{2} - i\sin\frac{\delta}{2}\cos 2R \end{pmatrix},$$

where $\delta = \beta_e L$ is the phase difference between the light waves passing along the slow and fast birefringence axes; $\beta_e = (\beta^2 + \beta_c^2)^{1/2}$ is the elliptic birefringence of the SMF; L is the length of the SMF contour; and the parameter R characterizes the ellipticity of polarization eigenmodes of the SMF. As indicated above, $\tan R = b/a$, where a and b are the larger and smaller axes of the polarization ellipse. If $R = 0$, the SMF polarization modes are linear, and if $R = \pi/4$, they are circular.

We note that Eqn (17) does not contain Jones matrices describing beam splitters in the FRI circuit (see Fig. 1). This is because the Jones matrix of an ideal polarization-isotropic all-fiber beam splitter is the identity matrix with the coefficient $1/\sqrt{2}$. The identity matrix can be ignored in calculations because the Jones vector multiplied by it does not change its form. The coefficient $1/\sqrt{2}$ can also be dropped because the light intensity to be calculated is a relative value, while the absolute values of the amplitudes of electric fields of counterpropagating waves do not affect the final result in calculations of the phase difference of the counterpropagating waves [this is demonstrated below, see Eqn (21)]. It is shown in what follows that if the FRI circuit uses discrete beam splitters — not all-fiber ones — then the phase difference between counterpropagating waves is affected quite significantly.

In the most general case, the expressions for the total light intensity at the FRI output and for the part of it that determines the intensity and phase difference of the interference signal are very complicated and cumbersome.[14] In the particular case of no rotation ($\Phi_S = 0$) and in the absence of polarizers in the FRI circuit ($\varepsilon = 1$), the corresponding expressions are considerably simplified:

$$I_{full} = |\mathbf{E}^+ + \mathbf{E}^-|^2 = 2\left[2 - \cos^2(2R)\sin^2(\alpha_2 + \alpha_1)\right], \tag{18}$$

$$I_{interf} = \mathrm{Re}\,(E_x^+ E_x^{-*} + E_y^+ E_y^{-*}) = 1 - \cos^2(2R)\sin^2(\alpha_2 + \alpha_1), \tag{19}$$

$$\begin{aligned} \mathrm{Im}\,(E_x^+ E_x^{-*} + E_y^+ E_y^{-*}) &= \cos(2R)\sin(\alpha_2 + \alpha_1) \\ &\times \left[(A_y^2 - A_x^2)\sin(2R)\cos(\alpha_2 - \alpha_1)\right. \\ &+ 2A_x A_y\left(\cos(2R)\cos(\alpha_2 + \alpha_1)\sin\psi\right. \\ &\left.\left. + \sin(2R)\sin(\alpha_2 - \alpha_1)\cos\psi\right)\right]. \end{aligned} \tag{20}$$

We note that the NPDCW of the counterpropagating waves at the output of the fiber ring interferometer due to PN1 is given by the formula

$$\varphi_{non} = \arctan\frac{\mathrm{Im}\,(E_x^+ E_x^{-*} + E_y^+ E_y^{-*})}{\mathrm{Re}\,(E_x^+ E_x^{-*} + E_y^+ E_y^{-*})} . \tag{21}$$

We need these expressions in the discussion of the experiments conducted to observe the geometric phase in FRI [26–28].

6.2 Nonreciprocal geometric phase of counterpropagating waves in FRIs

The condition $L \gg l_{dep}$ is practically always satisfied in FRIs with nonmonochromatic radiation sources. Hence, as mentioned above, the counterpropagating waves traveling along different birefringence axes of the SMF in the absence of random inhomogeneities in the fiber lightguide interfere only

[13] In the absence of a polarizer in the FRI circuit, the orientation of the axes of the Cartesian coordinate system is chosen arbitrarily.

[14] A detailed analysis of these expressions is a topic for a separate work [145]. We note that in the case of an imperfect (nonideal) polarizer ($0 \leqslant \varepsilon \leqslant 1$) in the FRI circuit, the results obtained in [145] show that the polarization nonreciprocity effect is not 'hidden' or 'virtual' as assumed above [16, 22, 23], because light intensity at the FRI output is a function of the phase difference ψ between the orthogonal components of the electric field vector at the FRI input.

pairwise. Therefore, we can consider two independent interference patterns at the FRI output and, correspondingly, two independent and generally nonidentical NPDCWs caused by PN1,

$$\varphi_{\rm non}^{(1,2)} = \arctan \frac{\operatorname{Im}(E_{x,y}^{+} E_{x,y}^{-*})}{\operatorname{Re}(E_{x,y}^{+} E_{x,y}^{-*})} . \qquad (22)$$

It was suggested [24] that these phases can be calculated using the Poincaré sphere technique. As shown in Ref. [24] (see also Ref. [146]), the NPDCW for each of the SMF axes (slow or fast) equals half the solid angle, with its apex at the origin of coordinates, subtended by the spherical triangle on the Poincaré sphere determined by the following three points: the point corresponding to the RP state at the input to the FRI circuit; the point corresponding to the RP state on one of the outputs of the FRI contour; and the point corresponding to the RP state at the opposite output of the FRI contour. Obviously, the point on the Poincaré sphere representing the RP state of the FRI contour input is common for both spherical triangles that correspond to the slow and fast axes of the SMF contour. The nonreciprocal phase differences discussed here are defined on the Poincaré sphere, and we therefore deal with a manifestation of geometric phases. It was proposed in Ref. [146] to refer to them as nonreciprocal geometric phases of counterpropagating waves (NGPCWs). The NGPCW for counterpropagating waves traveling along the slow axis of the SMF contour equals $\varphi_{\rm non}^{(1)}$, and that for the fast axis equals $\varphi_{\rm non}^{(2)}$.

We consider an NGPCW in a simple particular case: polarization eigenmodes of the SMF contour of the FRI are linear, and the slow axes of linear birefringence of the SMF at the contour input rotate by the angles α_1 and α_2 (see Fig. 10). There is no polarizer in the FRI circuit, and the RP state at the FRI input is right-circular. Figure 11 shows a spherical triangle ABN on the Poincaré sphere for the slow birefringence axis OBC (the second triangle $A'B'N$ for the fast axis OBC, where points A' and B' are diametrically opposite to points A and B, is not shown in Fig. 11). Point N corresponds to the right-circular polarization of light at the FRI input and points A and B correspond to the RP state at the FRI outputs. The angle $2\alpha_1$ is counted along the Poincaré sphere equator in the reverse direction because the angle α_1 is measured counterclockwise in real space (see Fig. 10). The NGPCW is numerically equal to half the solid angle subtended by the spherical triangle ABN or, for a unit-radius Poincaré sphere, equals half the ABN area. Clearly, if linearly polarized light is sent to the FRI input, then both triangles degenerate to arcs (parts of the Poincaré sphere equator) and the NGPCWs equal zero for both polarization modes.

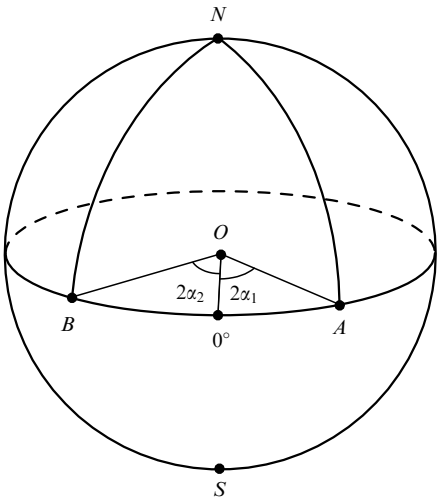

Figure 11. Representation of the nonreciprocal geometric phase of counterpropagating waves (NGPCW) on the Poincaré sphere. Point N corresponds to circular polarization of nonmonochromatic light at the FRI input and points A and B correspond to linear polarizations of counterpropagating waves traveling along the slow axis of linear birefringence of the SMF of the FRI contour, with azimuths α_1 and α_2.

Another, equivalent definition of the NPDCW can be proposed. In the particular case shown in Fig. 11, we consider two open figures, each formed by two arcs on the Poincaré sphere: the first by NA and AB and the second by NB and BA. These arcs have the following physical interpretation. At one of the inputs of the contour, the circularly polarized light has excited a slow linearly polarized mode of the SMF, corresponding to the arc NA. Because the orientations of the axes at the input to the contour are different, this means that the SMF is to some extent twisted and its polarization modes are Ginzburg's screw polarization modes (GSPMs), and in this case they are practically linear. At the output of the contour, a GSPM rotates by the angle $\alpha_1 - \alpha_2$, which corresponds to the arc AB. Similarly, for the counterpropagating waves, we can consider the arcs NB and BA. Even though each of the figures ABN and NBA is open, they form a spherical triangle together. Therefore, the NGPCW is numerically equal to half the solid angle subtended by the spherical triangle on the Poincaré sphere formed by arcs corresponding to the excitation and the evolution of Ginzburg's screw polarization modes on the FRI contour.

It may seem at first glance that the NGPCW is identical to the PP1 because both are determined by the area of spherical triangles on the Poincaré sphere. This is not true, however, First, the PP1 is numerically equal to the difference between π and half the area of the complementary triangle ABC', not to half the area of triangle ABC (see Fig. 2). Second (and this is the principal point), for the PP1, point C on the Poincaré sphere corresponds to the RP state that is the sum of RP states corresponding to points A and B on this sphere, while for the NGPCW, point N does not correspond to the sum of polarizations at points A and B (see Fig. 11): the sum of two linearly polarized light beams is also linearly polarized, while N corresponds to right-circular polarization. The physical factors causing the appearance of PP1 and the NGPCW are also different: PP1 is a consequence of the difference between the RP states of two beams not differing in kinematic phase, while the NGPCW is a consequence of the two beams (counterpropagating waves at the FRI output) having different initial phases, which they already acquired at the input to the contour owing to nonsimultaneous excitation.

The Poincaré sphere method [24] is not a universal tool for calculating $\varphi_{\rm non}$ due to polarization nonreciprocity of the NPDCW, nor for calculating PP2. The NGPCW of the waves traveling along the slow and fast axes of the SMF of the FRI contour [i.e., $\varphi_{\rm non}^{(1,2)}$, see formula (22)] are the arguments of two complex numbers, while $\varphi_{\rm non}$ [see formula (21)] is the argument of the complex number that is the sum of the two numbers above. In the general case, however, it is impossible to calculate the argument of the sum if we only know the arguments of the addends because the magnitudes of the addends must also be known. The NPDCW is identically equal to the NGPCW only in the FRI with a contour made of

a single-polarization singlemode optical fiber, because in this case only one spherical triangle corresponding to the unique polarization of counterpropagating waves is created on the Poincaré sphere. A number of particular cases where the NPDCW can be calculated when the NGPCW is known were discussed in Ref. [24]. In the general case, however, the calculations that do not involve the phase difference of the counterpropagating waves not caused by rotation of anisotropy axes must be carried out by the Jones matrix techniques. Nevertheless, the Poincaré sphere technique may prove very useful for a simple and visually clear presentation of the polarization nonreciprocity phenomenon and for a straightforward synthesis of situations not resulting in polarization nonreciprocity. This is discussed in detail in Refs [24, 146]. For instance, it is shown in Ref. [24] that in the case of circularly polarized modes in the SMF of the fiber ring interferometer contour, the NGPCW of either polarization mode is zero, and therefore the NPDCW is also zero.

The main conclusions of this section are as follows. First, the NGPCW can be regarded as a consequence of the differences between the conditions of excitation and evolution of Ginzburg's screw polarization modes on the Poincaré sphere. Second, in the general case, it is advisable to conduct the calculation of the NPDCW using the Jones matrix technique or the method of field expansion in normal waves [101 – 103]. In general, the Poincaré sphere method allows giving a clear illustration of the phenomenon of polarization nonreciprocity. In a number of important particular cases, the NPDCW equals the NGPCW.

7. Analysis of experiments on recording the geometric phase in FRIs

We now consider the results of experiments [26 – 28] that recorded changes in the phase on the interference pattern [26] and in light intensity [27, 28] at the FRI output in response to a change in the pitch of the helicoidal winding of a singlemode fiber lightguide.

7.1 Parameters of fiber ring interferometers on which measurements were conducted

FRIs investigated in Refs [26 – 28] had SMF contours with weak birefringence and no polarizer. The FRI circuit in Ref. [26] had a single beam splitter, namely, a discrete optical element — a polarization-isotropic beam-splitting prism, while part of the SMF contour was one half of the SMF loop ($d = 125$ μm) wound onto a spool 23 cm in diameter. The FRI circuit in Refs [27, 28] contained two all-fiber beam splitters and two turns of the SMF on the spool (neither the diameters of the SMF and the spool nor the total length of the SMF were reported). However, using the dependence of the angle of rotation of the light polarization plane (the Rytov angle) on the winding pitch given in Ref. [28], we can make a numerical evaluation using formula (12), which indicates that the spool diameter was approximately 13 cm. The dichroism of beam splitters in Refs [26 – 28] was negligibly small. Monochromatic light sources with a linear RP state were used in Refs [26 – 28]: an He-Ne laser ($\lambda = 0.63$ μm) in Ref. [26], with the RP state at the output nearly linear and changing to circular after passing through a polarizer and a quarter-wave plate; and a semiconductor laser ($\lambda = 1.3$ μm) in Ref. [28], with an RP state that could be varied arbitrarily using the so-called Lefevre polarization controller [105] that consisted of two SMF rings with birefringence induced by bending. A nonmonochromatic nonpolarized superfluorescent light source ($\lambda = 1.5$ μm, linewidth $\Delta\lambda = 50$ nm) was also used in Ref. [27]. Such radiation sources have very low polarization [147]. There was another RP state controller inside the FRI contour in Refs [27, 28] in which the value of linear birefringence in the SMF was controlled through mechanical compression [148]. Using this controller, a segment of the lightguide was created, equivalent to the half-wave phase plate. In Refs [26 – 28], the lightguide was placed in a Teflon tube and could easily unwind as the pitch of the helicoidal winding was varied. In Ref. [26, 27], the pitch of helicoidal winding was varied by shifting one of the ends of the helix, and in Ref. [28], by symmetrically shifting both ends of the winding in opposite directions.

Special sampling measurements conducted in Refs [26, 28] showed that birefringence in the SMF was practically unaffected by varying the pitch of the helicoidal winding. Using formula (10), it was possible to calculate linear birefringence induced by winding the SMF onto the spool. It is likely that a standard lightguide with the diameter $d = 125$ μm was used in Refs [27, 28].

In this case, we have $\beta = 0.425$ rad m^{-1}, $\Delta n = 4 \times 10^{-8}$ for experiments in Ref. [26], and $\beta = 0.51$ rad m^{-1}, $\Delta n = 1.2 \times 10^{-7}$ in Refs [27, 28]. Because the residual difference between refractive indices along the slow and fast axes in weakly anisotropic SMFs is typically $\Delta n \sim 10^{-6} - 10^{-7}$, we can assume that the winding of the SMF onto the spool [26 – 28] indeed caused very little increase in linear birefringence.

Here, we need to point to one specific feature of the FRI circuit used in Ref. [26], which is important for interpreting the results of this experiment. As mentioned above, the experiment in Ref. [26] used a beam-splitting prism whose Jones matrix, in contrast to the Jones matrix of an all-fiber beam splitter, is not the identity matrix but is given by

$$\frac{1}{\sqrt{2}}\begin{pmatrix} 1 & 0 \\ 0 & -1 \end{pmatrix}.$$

For example, if a beam with the right-circular polarization is incident on this prism, the beam passing through the beam-splitter prism does not change its RP state, while the beam reflected from it becomes left-polarized, that is, changes the sign of circular polarization. The sign of circular polarization of the beam reflected from a polarization-isotropic mirror is changed in the same way. If the SMF of the contour has its circularly polarized eigenmodes, then one counterpropagating wave has right-circular polarization and the other left-circular polarization. The counterpropagating waves again acquire identical circular polarizations at the FRI output because one passes through a beam-splitter prism and the other is reflected by it.

In principle, the FRI investigated in Ref. [26] can be regarded as the so-called polarization FRI (PFRI, see Section 5.7 of review [16]), in which one counterpropagating wave travels along the slow axis of the SMF contour and the other along the fast axis. Earlier PFRIs contained a polarization prism at the input, in order to excite various mutually orthogonal linear polarizations in counterpropagating waves [100, 149 – 154]. PFRIs were designed to detect nonreciprocal effects [100, 149, 150] and gravitation waves [151 – 154]. Therefore, a PFRI with the conventional beam-splitter prism for geometric phase measurements was first proposed in Ref. [26].

7.2 Analysis of experimental results

We note first of all that because the areas of the FRI contours investigated in Refs [26 – 28] were small, the influence of the Sagnac effect on the phase difference between counterpropagating waves due to the earth's rotation is negligible [see formula (16)]. We also note that only one of the possible mechanisms producing changes in the NPDCW (observed experimentally in Ref. [26]) and in the value of I_{full} (observed experimentally in Refs [27, 28]) was discussed in [29], namely the effect of changed birefringence of the SMF in response to the changed pitch of the helicoidal winding of the lightguide. Here, we discuss the results reported in Refs [26 – 28] from a more general standpoint.

The effect recorded in Ref. [26] was a shift in the positions of fringes formed by interference of counterpropagating waves at the FRI output in response to the changed pitch of the helicoidal winding of the singlemode fiber lightguide in an FRI with a monochromatic light source and circular RP state. As mentioned above, one of the counterpropagating waves was traveling along the right-circular birefringence axis of the SMF, and the other along the left-circular one. Both waves acquired identical polarization at the output and formed an interference pattern. Because the circular birefringence of the SMF contour arises as a result of the Rytov effect, and there was a circular RP state at the FRI input, the phase difference between counterpropagating waves was numerically equal to twice the Rytov – Vladimirskiĭ phase because one wave acquired the RV phase with the positive sign, and the other with the negative one. Hence, the FRI circuit [26] made it possible to observe the polarization nonreciprocity due to the Rytov effect. In this case, the nonreciprocity occurred because of the presence of two channels, that is, the Rytov effect resulted in PN2.

Because a discrete beam-splitter, not an all-fiber one, was used in Ref. [26], a certain phase mismatch of wave fronts of counterpropagating waves could also occur in principle. In this case, if there was sufficient linear birefringence in the SMF, and its polarization eigenmodes could be not quite circular, then the change in the Rytov angle in response to the changed pitch of the helicoidal winding of the lightguide could result in a certain change φ_{non} of the NPDCW as a result of the changed PN1, and this could also lead to a shift of interference fringes at the FRI output.

The quantity monitored in Refs [27, 28] was the change in the value I_{full} as the pitch of the helicoidal winding was varied; the FRI used a monochromatic light source. In this case, if the polarization eigenmodes of the SMF of the FRI contour are linear ($R = 0$), then the total intensity of radiation at the output of the FRI without a polarizer is described by the expression

$$I_{\text{full}} = \cos^2 \frac{\alpha_{\text{Ryt}}}{2} , \qquad (23)$$

where α_{Ryt} stands for Rytov angle (13). As follows from Eqn (23), the value of I_{full} is then independent of the RP state at the FRI input, which is in agreement with the results of measurements [27, 28]. In this situation, the change in the Rytov angle in response to the changed pitch of lightguide winding resulted in changed PN1 and PN2, and the contributions of the two can hardly be separated.

As shown above, there are no nonreciprocal effects shown by the two-channel type of FRI if the radiation source is nonmonochromatic; hence, it is most interesting to analyze the results of experiments [27] because they allow ignoring changes in the PP2 and RV phase in response to the changed pitch of the helicoidal winding.

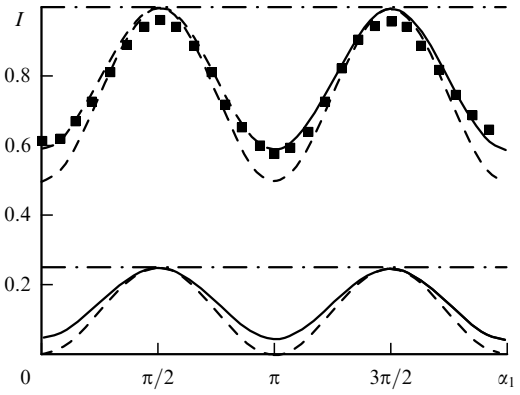

Figure 12. The total light intensity I_{full} (the upper group of curves) and the interference light intensity I_{interf} (the lower group of curves) at the FRI output as functions of the azimuth α_1 of the SMF axis at the input to the first beam-splitter in the FRI. $\varepsilon = 1$, $\alpha_2 = \pi/2$, $R = 0$ (dashed curves), $R = \pi/14$ (solid curves), $R = \pi/4$ (dash-dot curves). Dots mark experimental data [27].

In Ref. [27], the total light intensity I_{full} was measured at the output of the first and second beam splitters (see Fig. 1). In actual FRIs, the signal is always measured at the output of the first beam splitter because the signal at the output of the second beam splitter (located at the input to the contour) has an additional phase difference between the counterpropagating waves: one wave passes through it twice, while the other is twice reflected from it. Hence, in what follows, we always consider only the function I_{full} at the output of the first beam splitter (this is illustrated in Ref. [27] by the upper plot in Fig. 4). The part of the SMF in the FRI contour that is wound on a spool has circular birefringence due to the Rytov effect. The remaining part of the lightguide contour, with the exception of the compressed segment with linear birefringence, can be considered practically isotropic. Therefore, because the change in the pitch of the helicoidal winding of the SMF was produced in Ref. [27] by shifting only one of the two ends of the lightguide coil, one of the angles, α_1 or α_2 (to be specific, we assume that $\alpha_1 = \alpha_{\text{Ryt}}$), changes in expression (18) for I_{full} because of the changing magnitude of the Rytov effect.

Figure 12 plots the light intensity I_{full} as a function of the rotation angle α_1 as calculated in accordance with Eqn (18). The calculations assumed the polarizer coefficient in the FRI circuit $\varepsilon = 1$, and the value of ellipticity of Ginzburg's screw polarization modes for the equivalent uniform SMF of the contour was $R = 0, \pi/14, \pi/4$.[15] As in the case with a monochromatic radiation source, the quantities A_x, A_y and the phase difference ψ between the electric field components at the FRI input did not affect the behavior of the curve $I_{\text{full}}(\alpha_1)$. This indicates that the RP state does not change $I_{\text{full}}(\alpha_1)$, which is in good agreement with the experimental

[15] The FRI contour [27, 28] consisted of a number of different segments of the SMF: weakly birefringent leading segments, a compressed segment with linear birefringence, and a segment of helicoidal winding with equivalent circular birefringence. However, in the absence of data on the length of each of these segments and on the value of nonperturbed birefringence of the SMF, we were forced to replace it with a certain equivalent uniform SMF, that is, in fact, with a discrete optical element.

conditions in Ref. [27], where light at the FRI input was depolarized. Figure 12 also plots experimental values of I_{full} taken from paper [27]. We see that the experimental values fit well the theoretical curve calculated in accordance with Eqn (18) for $R = \pi/14$. For the sake of comparison, Fig. 12 gives the function $I_{\text{full}}(\alpha_1)$ in the case of linear ($R = 0$) and circular ($R = \pi/14$) GSPMs in the singlemode fiber lightguide contour of the FRI. We see that the curves do not agree with the experimental values given in Ref. [27].

We therefore see that in Ref. [27], the Rytov effect in a fiber ring interferometer was experimentally observed, resulting in a change of the azimuth of one of the SMF axes at the contour input in response to changes in the pitch of the helicoidal winding. At the same time, using Eqn (18), we were able to calculate the ellipticity of Ginzburg's screw polarization modes in the SMF in paper [27]: $R = \pi/14$, that is, the ratio of the smaller axis of the ellipse to the larger axis was $\tan R = 0.228$. The reason why the GSPMs in the SMF in Ref. [27] had certain ellipticity was most likely the compressed segment of the lightguide; however, it could also be related to the residual torsional strain in the light guide. If the contour of the experiment in Ref. [27] contained no compressed segment of the SMF equivalent to a half-wave linear phase plate, then the GSPMs would be very nearly circular ($R \sim \pi/4$) and the changes in the output intensity due to the Rytov effect would be practically unobservable.

We note that the Rytov effect also changes the Rytov angle and, therefore, the NPDCW, which is related to PP2.

We thus see that experiment [26] observed the Rytov–Vladimirskiĭ (RV) phase in the fiber ring interferometer, and experiments [27, 28] observed the Rytov effect in the FRI. The authors of Ref. [26] give the correct interpretation to their experimental results but refer to the RV phase as Berry's phase. The authors of Refs [27, 28] also correctly indicate that changes in light intensity of the FRI output were caused by the rotation of the polarization plane in response to the changed pitch of the helicoidal winding of the fiber optics lightguide, but they add to this that they record the changes in Berry's phase even though they actually measured changes in the Rytov angle. However, because both the Rytov angle and the Ishlinskii angle in classical mechanics are classified as geometric phases in the broader sense, they can in principle be referred to as Berry's phases. But this very general name for distinct types of geometric phases may make it more difficult to interpret the results of various studies, and we therefore find it advisable to indicate the specific geometric phase each time.[16]

The main conclusion of this section is that what is actually measured in experiments with controlled pitch of helicoidal winding of the singlemode fiber lightguide of the FRI is the Rytov effect in the case of nonmonochromatic light sources, while in the case of monochromatic light sources, the change in the Rytov–Vladimirskiĭ phase is additionally recorded.

8. Unfounded hypotheses related to geometric phases in FRIs

The existence of geometric phases in optics led authors of some publications to wrong conclusions about the functioning of fiber ring interferometers. For instance, we read in Refs [155–158] that the magnitude of the Sagnac effect in FRIs depends on the type of winding (stacking) of the SMF contour onto the spool; these authors also discuss the possibility of a significant increase in the phase difference between counterpropagating waves in view of the rotation of the polarization plane in the case of nonplanar (e.g., toroidal) winding of SMFs. E I Yakubovich proved this statement false by using the eikonal method in paper [29] written together with one of the authors of the present review. Furthermore, it was shown in Ref. [29] that the value of the phase difference between counterpropagating waves due to the Sagnac effect is proportional to the area of the projection of the contour outline onto the plane orthogonal to the rotation axis. Hence, it is maximal if the FRI contour has a planar winding and cannot be increased by the noncoplanarity of the contour outline: the phase difference can only decrease in this case.

As was shown in Section 7, the Rytov effect due to noncoplanarity of winding the SMF contour of the FRI can result in two effects:

(1) The change in the Rytov angle may result in a changed NPDCW, which is related to PN1 (i.e., to nonsimultaneity of excitation of counterpropagating waves in FRIs).

(2) For a nonmonochromatic radiation source, the appearance of the RV phase results in the appearance of the NPDCW, which is related to PN2 (i.e., to the two-channel situation).

The Rytov angle can thus only result in the rise or modification of the magnitude of the NPDCW in fiber ring interferometers, that is, can only produce an additive term in the phase difference caused by rotation (the Sagnac effect). There can be no question of increasing the sensitivity of the Rytov effect to rotation.

9. Conclusion

We now formulate the main results of this study.

(1) The Rytov effect, that is, the rotation of the light polarization plane resulting from free noncoplanar winding of a singlemode fiber lightguide, converts polarization eigenmodes of the SMF into Ginzburg's screw polarization modes (GSPMs); however, no additional elliptic birefringence is generated in the process. The Rytov effect in SMFs is therefore a manifestation of optical activity not accompanied by a modification of birefringence in the helical coordinate system.

(2) The Rytov–Vladimirskiĭ phase has a geometric optics origin, and therefore is a form of geometric phase; at the same time, it can be regarded as a manifestation of dynamic phases because it is defined for a circular radiation polarization state in the case where the optical activity is caused by the Rytov effect.

(3) In the general case, geometric phases in optics, defined on the Poincaré sphere, do not allow calculating the actual phase change corresponding to the change in the RP state over a segment of an SMF or FRI. For instance, the Pancharatnam phase PP2 does not in general correspond to the actual phase even in the case of cyclic evolution of the RP state in a medium with an arbitrary type of birefringence, for instance, if both polarization eigenmodes were excited with unequal weights. In the general case, the NGPCW of a fiber ring interferometer does not allow calculating the nonreciprocal geometric phase of counterpropagating waves caused by PN1. Nevertheless, geometric phases make it possible to

[16] I A Andronova made a significant contribution to the interpretation of the results reported in Refs [26–28].

give a simpler and visually clear illustration of various polarization effects in SMFs of a fiber ring interferometer.

(4) The reason why geometric phases in polarization optics do not always correspond to the actual changes in the light phase is that they always arise during the process of light propagation through anisotropic optical media and cannot always be separated from conventional kinematic and dynamic phases, in contrast to geometric phases of classical mechanics, where it is always possible to separate the translational motion of a solid from its rotational and conical motion.

(5) The calculation of the actual phase change of light in the SMF or of the NPDCW due to polarization nonreciprocity in FRIs should be carried out in the general case by the Jones matrix technique even though using GSPMs may prove advantageous in specific cases.

(6) In media possessing no magnetic activity or possessing simultaneous natural activity and linear birefringence, the Pancharatnam phase PP2 and the Rytov – Vladimirskiĭ phase are reciprocal and can be observed within a segment of the SMF or in Michelson and Mach – Zender fiber interferometers; in fiber ring interferometers, they can be observed only in two-channel situations that arise if a monochromatic radiation source is used, that is, as a manifestation of a change in PN2.

(7) The NGPCW can be regarded as a consequence of the difference between the excitation and evolution condition for GSPMs in the singlemode fiber lightguide of the fiber ring interferometer, corresponding to different arcs on the Poincaré sphere. If the FRI contour is made of a single-polarization SMF, then the NGPCW and NPDCW are identical.

We were able to establish that specific changes caused by the Rytov effect in the radiation polarization state of light propagating along a helicoidal beam were first treated in Ref. [159]. The effect of waveguide twisting on the generation of geometric phases in the microwave range was discussed by L A Rivlin in Ref. [160]. We note that polarization eigenmodes of such waveguides are Ginzburg's screw polarization modes.

In conclusion, the authors express their gratitude to V L Ginzburg and V V Vladimirskiĭ for a discussion of their results published in the 1940s, to Vl V Kocharovskiĭ for a discussion the results, which led to a number of important changes and a considerable improvement in the presentation of the material, to V M Gelikonov, Yu I Neĭmark, G V Permitin, and S A Kharlamov for a number of useful suggestions, and to S N Novikova for her help in preparing graphic illustrations. This work was partly supported by the Russian Foundation for Basic Research grant No. 03-02-17253 and partly by the grant No. NSh 1622.2003.2.

References

1. Berry M V *Proc. R. Soc. London Ser. A* **392** 45 (1984)
2. Vinitskiĭ S I et al. *Usp. Fiz. Nauk* **160** (6) 1 (1990) [*Sov. Phys. Usp.* **33** 403 (1990)]
3. Anandan J *Nature* **360** 307 (1992)
4. Klyshko D N *Usp. Fiz. Nauk* **163** (11) 1 (1993) [*Phys. Usp.* **36** 1005 (1993)]
5. Toronov V Yu, Derbov V L, Priyutova O M *Izv. Vyssh. Uchebn. Zaved. Prikl. Nelin. Dinamika* **4** (6) 3 (1996)
6. Bodnarchuk V I, Davtyan L S, Korneev D A *Usp. Fiz. Nauk* **166** 185 (1996) [*Phys. Usp.* **39** 169 (1996)]
7. Malykin G B *Usp. Fiz. Nauk* **167** 337 (1997) [*Phys. Usp.* **40** 317 (1997)]
8. Rytov S M *Dokl. Akad. Nauk SSSR* **18** 263 (1938)
9. Rytov S M *Tr. Fiz. Inst. Akad. Nauk SSSR* **2** (1) 41 (1940)
10. Vladimirskii V V *Dokl. Akad. Nauk SSSR* **31** 222 (1941)
11. Pancharatnam S *Proc. Ind. Acad. Sci. A* **44** 247 (1956); reprinted in *Collected Work of S. Pancharatnam* (Ed. G W Series) (London: Oxford Univ. Press, 1975)
12. Pancharatnam S *Proc. Ind. Acad. Sci. A* **44** 398 (1956); reprinted in *Collected Work of S. Pancharatnam* (Ed. G W Series) (London: Oxford Univ. Press, 1975)
13. Hamilton W R *Lectures on Quaternions* (Dublin: Hodges and Smith, 1853) p. 338
14. Ishlinskiĭ A Yu *Mekhanika Spetsial'nykh Giroskopicheskikh Sistem* (Mechanics of Special Gyroscopic Systems) (Kiev: Izd. Akad. Nauk USSR, 1952)
15. Ishlinskiĭ A Yu *Mekhanika Giroskopicheskikh Sistem* (Mechanics of Gyroscopic Systems) 2nd ed. (Moscow: Izd. Akad. Nauk SSSR, 1963)
16. Andronova I A, Malykin G B *Usp. Fiz. Nauk* **172** 849 (2002) [*Phys. Usp.* **45** 793 (2002)]
17. Logunov A A, Chugreev Yu V *Usp. Fiz. Nauk* **156** 137 (1988) [*Sov. Phys. Usp.* **31** 861 (1988)]
18. Malykin G B, Kharlamov S A *Usp. Fiz. Nauk* **173** 985 (2003) [*Phys. Usp.* **46** 957 (2003)]
19. Vugal'ter G A, Malykin G B *Izv. Vyssh. Uchebn. Zaved. Radiofiz.* **42** 373 (1999)
20. Malykin G B *Usp. Fiz. Nauk* **170** 1325 (2000) [*Phys. Usp.* **43** 1229 (2000)]
21. Malykin G B *Usp. Fiz. Nauk* **172** 969 (2002) [*Phys. Usp.* **45** 907 (2002)]
22. Andronova I A, Gelikonov G V, Malykin G B *Kvantovaya Elektron.* **26** 271 (1999) [*Quantum Electron.* **26** 271 (1999)]
23. Andronova I A, Gelikonov G V, Malykin G B *Proc. SPIE* **3736** 423 (1999)
24. Malykin G B *Opt. Spektrosk.* **81** 474 (1996) [*Opt. Spectrosc.* **81** 431 (1996)]
25. Berestetskiĭ V B, Lifshitz E M, Pitaevskiĭ L P *Kvantovaya Elektrodinamika* (Quantum Electrodynamics) (Moscow: Nauka, 1989) [Translated into English (Oxford: Pergamon Press, 1982)]
26. Frins E M, Dultz W *Opt. Commun.* **136** 354 (1997)
27. Senthilkumaran P, Thursby G, Culshaw B *Opt. Lett.* **25** 533 (2000)
28. Senthilkumaran P, Culshaw B, Thursby G *J. Opt. Soc. Am. B* **17** 1914 (2000)
29. Yakubovich E I, Malykin G B *Izv. Vyssh. Uchebn. Zaved. Radiofiz.* **45** 975 (2002) [*Radiophys. Quantum Electron.* **45** 895 (2002)]
30. Ross J N *Opt. Quantum Electron.* **16** 455 (1984)
31. Galanin A D *J. Phys. USSR* **6** 35 (1942)
32. Kravtsov Yu A, Orlov Yu I *Geometricheskaya Optika Neodnorodnykh Sred* (Geometric Optics of Inhomogeneous Media) (Moscow: Nauka, 1980) [Translated into English (Berlin: Springer-Verlag, 1990)]
33. Kline M, Kay I W *Electromagnetic Theory of Geometrical Optics* (New York: John Wiley & Sons, 1965)
34. Lewis R M *IRE Trans.* **AP-14** 100 (1966)
35. Tang C H *IEEE Trans.* **MTT-18** 69 (1970)
36. Born M, Wolf E *Principles of Optics* (Oxford: Pergamon Press, 1969) [Translated into Russian (Moscow: Nauka, 1973)]
37. Smirnov A I, Fraĭman G M *Zh. Eksp. Teor. Fiz.* **83** 1287 (1982) [*Sov. Phys. JETP* **56** 737 (1982)]
38. Haldane F D M *Opt. Lett.* **11** 730 (1986)
39. Berry M V *Nature* **326** 277 (1987)
40. Kitano M, Yabuzaki T, Ogawa T *Phys. Rev. Lett.* **58** 523 (1987)
41. Shurkliff W A *Polarized Light* (Cambridge, Mass.: Harvard Univ. Press, 1962) [Translated into Russian (Moscow: Mir, 1965)]
42. Malykin G B *Izv. Vyssh. Uchebn. Zaved. Radiofiz.* **40** 265 (1997) [*Radiophys. Quantum Electron.* **40** 175 (1997)]
43. Markovski B, Vinitsky V (Eds) *Topological Phase in Quantum Theory* (Singapore: World Scientific, 1989)
44. Shapere A, Wilczek F (Eds) *Geometric Phase in Physics* (Adv. Series in Math. Phys., Vol. 5) (Singapore: World Scientific, 1989)
45. Berry M V *J. Mod. Opt.* **34** 1400 (1987)
46. Berry M V *Phys. Today* **43** (12) 34 (1990)
47. Vali V, Shorthill R W *Appl. Opt.* **15** 1099 (1976)
48. Vali V, Shorthill R W *Appl. Opt.* **16** 290 (1977)

49. Logozinskiĭ V N "Study of glass fiber interferometer as angular velocity sensor", Graduation Project (Moscow: MFTI, 1979)
50. Ulrich R, Johnson M *Opt. Lett.* **4** 152 (1979)
51. Schiffner G et al. *Appl. Opt.* **18** 2096 (1979)
52. Schiffner G "Interferometer mit einer Spule aus einem Einmode-Wellenleiter", Patentschrift DE 2804103 C2 (FRG) 02.08.1979, Anmeldetag 31.01.1978
53. Schiffner G "Interferometer with a single-mode waveguide coil", US Patent No. 4259016. 31.03.1981, Filed 31.01.1979
54. Schiffner G "Interferometer with a single-mode waveguide coil", US Patent No. 4325636. 20.04.1982, Filed 11.01.1979
55. Gordon S A, Logozinskiĭ V N, Novikov A G *Kvantovaya Elektron.* **7** 2352 (1980) [*Sov. J. Quantum Electron.* **10** 1312 (1980)]
56. Ulrich R *Opt. Lett.* **5** 173 (1980)
57. Kintner E C *Opt. Lett.* **6** 154 (1981)
58. Böhm K et al. *Opt. Lett.* **6** 64 (1981)
59. Pavlath G A, Shaw H J *Appl. Opt.* **21** 1752 (1982)
60. Böhm K, Petermann K, Weidel E *J. Lightwave Tech.* **LT-1** 71 (1983)
61. Fridricks R J, Ulrich R *Electron. Lett.* **20** 330 (1984)
62. Burns W K, Moeller R P *J. Lightwave Tech.* **LT-2** 430 (1984)
63. Kozel S M et al. *Opt. Spektrosk.* **59** 180 (1985) [*Opt. Spectrosc.* **59** 106 (1985)]
64. Jones E, Parker J W *Electron. Lett.* **22** 54 (1986)
65. Tai S et al. *Electron. Lett.* **22** 546 (1986)
66. Kozel S M et al. *Opt. Spektrosk.* **61** 1295 (1986) [*Opt. Spectrosc.* **61** 814 (1986)]
67. Itoh K, Saitoh T, Ohtsuka Y *J. Lightwave Tech.* **LT-5** 916 (1987)
68. Mortimore D B *J. Lightwave Tech.* **6** 1217 (1988)
69. Birks T A, Morkel P *Appl. Opt.* **27** 3107 (1988)
70. Listvin V N *Opt. Spektrosk.* **67** 1208 (1989) [*Opt. Spectrosc.* **67** 712 (1989)]
71. Listvin V N *Izv. Vyssh. Uchebn. Zaved. Radiofiz.* **33** 458 (1990) [*Radiophys. Quantum Electron.* **33** 343 (1990)]
72. Fadeev A V *Izv. Vyssh. Uchebn. Zaved. Priborostroenie* **34** (8) 69 (1990)
73. Listvin V N, Logozinskiĭ V N *Izv. Vyssh. Uchebn. Zaved. Radiofiz.* **34** 1001 (1991) [*Radiophys. Quantum Electron.* **34** 791 (1991)]
74. Malykin G B *Izv. Vyssh. Uchebn. Zaved. Radiofiz.* **34** 817 (1991) [*Radiophys. Quantum Electron.* **34** 667 (1991)]
75. Malykin G B *Izv. Vyssh. Uchebn. Zaved. Radiofiz.* **35** 189 (1992) [*Radiophys. Quantum Electron.* **35** 134 (1992)]
76. Alekseev E I, Bazarov E N *Kvantovaya Elektron.* **19** 897 (1992) [*Sov. J. Quantum Electron.* **22** 834 (1992)]
77. Burns W K, Kersey A D *J. Lightwave Tech.* **10** 992 (1992)
78. Malykin G B *Opt. Spektrosk.* **75** 1314 (1993) [*Opt. Spectrosc.* **75** 775 (1993)]
79. Malykin G B *Opt. Spektrosk.* **76** 540 (1994) [*Opt. Spectrosc.* **76** 484 (1994)]
80. Malykin G B, Nefedov I M, Shereshevskiĭ I A *Izv. Vyssh. Uchebn. Zaved. Radiofiz.* **37** 1473 (1994) [*Radiophys. Quantum Electron.* **37** 847 (1994)]
81. Malykin G B et al. *Izv. Vyssh. Uchebn. Zaved. Radiofiz.* **37** 1567 (1994)
82. Malykin G B, Pozdnyakova V I, Pozdnyakov E L *Izv. Vyssh. Uchebn. Zaved. Radiofiz.* **38** 1293 (1995) [*Radiophys. Quantum Electron.* **38** 845 (1995)]
83. Blake J, Szafraniec B, Feth J *Opt. Lett.* **21** 1192 (1996)
84. Malykin G B *Opt. Spektrosk.* **83** 1013 (1997) [*Opt. Spectrosc.* **83** 937 (1997)]
85. Andronova I A et al. *Izv. Vyssh. Uchebn. Zaved. Radiofiz.* **40** 780 (1997)
86. Andronova I A, Gelikonov V M, Gelikonov G V *Izv. Vyssh. Uchebn. Zaved. Radiofiz.* **41** 1448 (1998)
87. Malykin G B, Pozdnyakova V I *Opt. Spektrosk.* **84** 145 (1998) [*Opt. Spectrosc.* **84** 131 (1998)]
88. Malykin G B, Pozdnyakova V I *Opt. Spektrosk.* **86** 505 (1999) [*Opt. Spectrosc.* **86** 444 (1999)]
89. Malykin G B, Pozdnyakova V I *Opt. Spektrosk.* **86** 513 (1999) [*Opt. Spectrosc.* **86** 451 (1999)]
90. Szafraniec B, Sanders G A *J. Lightwave Tech.* **17** 579 (1999)
91. Ruffin P B, Baeder J, Sung C C *Opt. Eng.* **40** 605 (2001)
92. Malykin G B, Pozdnyakova V I *Opt. Spektrosk.* **91** 130 (2001) [*Opt. Spectrosc.* **91** 119 (2001)]
93. Malykin G B *Opt. Spektrosk.* **91** 676 (2001) [*Opt. Spectrosc.* **91** 638 (2001)]
94. Malykin G B, Pozdnyakova V I *Radiotekh. Elektron.* **47** 633 (2002) [*J. Commun. Technol. Electron.* **47** 568 (2002)]
95. Malykin G B, Pozdnyakova V I *Opt. Spektrosk.* **94** 333 (2003) [*Opt. Spectrosc.* **94** 300 (2003)]
96. Vygodskiĭ M Ya *Spravochnik po Elementarnoĭ Matematike* (Handbook on Elementary Mathematics) (Moscow: Nauka, 1982)
97. Martinelli M, Vavassori P *Opt. Commun.* **80** 166 (1990)
98. Agranovich V M, Ginzburg V L *Kristallooptika s Uchetom Prostranstvennoĭ Dispersii i Teoriya Eksitonov* (Crystal Optics with Spatial Dispersion Taken into Account and Theory of Exitons) 2nd ed. (Moscow: Nauka, 1979) [Translated into English: *Crystal Optics with Spatial Dispersion, and Excitons* 2nd ed. (Berlin: Springer-Verlag, 1984)]
99. Novikov M A *Izv. Vyssh. Uchebn. Zaved. Radiofiz.* **32** 258 (1989)
100. Malykin G B *Opt. Spektrosk.* **80** 280 (1996) [*Opt. Spectrosc.* **80** 245 (1996)]
101. Ginzburg V L *Zh. Tekh. Fiz.* **14** 181 (1944)
102. Ginzburg V L *Rasprostranenie Elektromagnitnykh Voln v Plazme* (Propagation of Electromagnetic Waves in Plasma) (Moscow: GIFML, 1960) [Translated into English (New York: Gordon and Breach, 1962)]
103. Zheleznyakov V V, Kocharovskiĭ V V, Kocharovskiĭ Vl V *Usp. Fiz. Nauk* **141** 257 (1983) [*Sov. Phys. Usp.* **26** 877 (1983)]
104. Rashleigh S C, Ulrich R *Opt. Lett.* **3** 60 (1978)
105. Lefevre H C *Electron. Lett.* **16** 778 (1980)
106. Ulrich R, in *Fiber-Optic Rotation Sensors and Related Technologies: Proc. of the 1st Intern. Conf., Cambridge, Mass., USA, November 9–11, 1981* (Springer Ser. in Optical Sci., Vol. 32, Eds S Ezekiel, H J Arditty) (Berlin: Springer-Verlag, 1982) p. 52
107. Ulrich R, Simon A *Appl. Opt.* **18** 2241 (1979)
108. Barlow A J, Ramskov-Hansen J J, Payne D N *Appl. Opt.* **20** 2962 (1981)
109. Malykin G B, Pozdnyakova V I, Shereshevskiĭ I A *Opt. Spektrosk.* **88** 477 (2000) [*Opt. Spectrosc.* **88** 427 (2000)]
110. Marcuse D *Theory of Dielectric Optical Waveguides* (New York: Academic Press, 1974)
111. Marcuse D *Bell System Tech. J.* **54** 985 (1975)
112. Kaminow I P *IEEE J. Quantum Electron.* **QE-17** 15 (1981)
113. Rashleigh S C *J. Lightwave Tech.* **LT-1** 312 (1983)
114. Malykin G B, Pozdnyakova V I, Shereshevskiĭ I A *Opt. Spektrosk.* **83** 843 (1997) [*Opt. Spectrosc.* **83** 780 (1997)]
115. Kocharovskiĭ V V et al. *Izv. Ross. Akad. Nauk Ser. Fiz.* **62** 362 (1998)
116. Suvorov E V *Izv. Vyssh. Uchebn. Zaved. Radiofiz.* **14** 1320 (1972)
117. Azzam R M A, Bashara N M *Ellipsometry and Polarized Light* (Amsterdam: North-Holland Publ. Co., 1977) [Translated into Russian (Moscow: Mir, 1981)]
118. Poincaré H *Théorie mathématique de la lumière* Vol. II (Paris: G. Carré, 1892) p. 275
119. Wiener N *Acta Math.* **55** 117 (1930)
120. Jones R C *J. Opt. Soc. Am.* **31** 488 (1941)
121. Hurwitz H (Jr), Jones R C *J. Opt. Soc. Am.* **31** 493 (1941)
122. Jones R C *J. Opt. Soc. Am.* **31** 500 (1941)
123. Kataevskaya I V, Kundikova N D *Kvantovaya Elektron.* **22** 959 (1995) [*Quantum Electron.* **25** 927 (1995)]
124. Simson J K et al. *J. Lightwave Tech.* **LT-1** 370 (1983)
125. Bychkov A V et al., in *Tezisy Dokl. V Vsesoyuz. Konf.* "*Volokonno-Opticheskie Sistemy Peredachi*" (Abstracts of 5th USSR Conf. "Fiber Optics Communication Systems") (Moscow, 1988) Section 2, p. 42
126. Arutyunyan Z Yu et al., in *Tezisy Dokl. V Vsesoyuz. Konf.* "*Volokonno-Opticheskie Sistemy Peredachi*" (Abstracts of 5th USSR Conf. "Fiber Optics Communication Systems") (Moscow, 1988) Section 3, p. 7
127. Varnham M P, Birch R D, Payne D N, in *Proc. of the 5th Intern. Conf. on Integrated Optics and Optical Fiber Communication and 11th Europ. Conf. on Optical Communication* (Genova, Italy: Istituto Internazionale delle Communicazioni, 1985) p. 135
128. Tomita A, Chiao R Y *Phys. Rev. Lett.* **57** 937 (1986)
129. Frins E M, Dultz W *J. Lightwave Tech.* **15** 144 (1997)
130. Kharlamov S A, Private communication

131. Krobka N I, in *The 2nd Saint Petersburg Intern. Conf. on Gyroscopic Technology and Navigation, Saint Petersburg, 24 – 25 May 1995* Pt. II (St. Petersburg, 1995) p. 99
132. Kittel Ch, Knight W D, Ruderman M A *Berkeley Physics Course* Vol. 1 *Mechanics* (New York: McGraw-Hill, 1965) [Translated into Russian (Moscow: Nauka, 1975)]
133. Zhuravlev V F *Osnovy Teoreticheskoĭ Mekhaniki* (Foundations of Theoretical Mechanics) (Moscow: Nauka, 1997) p. 59
134. Malykin G B *Usp. Fiz. Nauk* **169** 585 (1999) [*Phys. Usp.* **42** 505 (1999)]
135. Malykin G B *Prikl. Mat. Mekh.* **63** 775 (1999) [*J. Appl. Math. Mech.* **63** 731 (1999)]
136. Zhuravlev V F *Prikl. Mat. Mekh.* **60** 323 (1996) [*J. Appl. Math. Mech.* **60** 319 (1996)]
137. Zhbanov Yu K, Zhuravlev V F *Izv. Akad. Nauk SSSR Mekh. Tverd. Tela* (1) 9 (1978)
138. Amel'kin N I *Izv. Ross. Akad. Nauk Mekh. Tverd. Tela* (2) 12 (2003)
139. Neĭmark Yu I, Fufaev N A *Dinamika Negolonomnykh Sistem* (Dynamics of Nonholomic Systems) (Moscow: Nauka, 1967) [Translated into English (Providence, RI: American Mathematical Soc., 1972)]
140. Malykin G B, Neĭmark Yu I *Pis'ma Zh. Tekh. Fiz.* **24** (11) 22 (1998) [*Tech. Phys. Lett.* **24** 421 (1998)]
141. Malykin G B, Neĭmark Yu I *Izv. Vyssh. Uchebn. Zaved. Radiofiz.* **41** 1125 (1998)
142. Malykin G B, Neĭmark Yu I *Zh. Tekh. Fiz.* **68** (11) 128 (1998) [*Tech. Phys.* **43** 1388 (1998)]
143. Emel'yanova I S, Malykin G B, in *Matematika i Kibernetika 2003: Yubileĭnaya Nauch.-Tekh. Konf. Fakul'teta VMK NNGU i NII PMK, Nizhniĭ Novgorod, 28 – 29 Noyabrya 2003 g.* (Mathematics and Cybernetics 2003. Collected papers of Special Conf. of the Dept of Computations and Cybernetics of Nizhniĭ Novgorod University and Research Institute of Applied Mathematics and Cybernetics, Nizhniĭ Novgorod, 28 – 29 November 2003) (Eds V P Savel'ev et al.) (Nizhniĭ Novgorod: Izd. NNGU, 2003) p. 139
144. Malykin G B, Pozdnyakova V I *Opt. Spektrosk.* **95** 646 (2003) [*Opt. Spectrosc.* **95** 603 (2003)]
145. Malykin G B, Pozdnyakova V I *Opt. Spektrosk.* **97** (2004) (in press)
146. Malykin G B *Opt. Spektrosk.* **84** 515 (1998) [*Opt. Spectrosc.* **84** 455 (1998)]
147. Alekseev E I et al. *Radiotekh. Elektron.* **41** 762 (1996)
148. Johnson M *Appl. Opt.* **18** 1288 (1979)
149. Novikov M A *Radiotekh. Elektron.* **21** 903 (1976)
150. Novikov M A *Opt. Spektrosk.* **61** 424 (1986) [*Opt. Spectrosc.* **61** 266 (1986)]
151. Sun K-X et al. *Phys. Rev. Lett.* **76** 3053 (1996)
152. Beyersdorf P T, Fejer M M, Byer R L *Opt. Lett.* **24** 1112 (1999)
153. Beyersdorf P T, Fejer M M, Byer R L *J. Opt. Soc. Am. B* **16** 1354 (1999)
154. Traeger S et al. *Opt. Lett.* **25** 722 (2000)
155. Staroverova M E, in *Proc. of the Intern. Conf.* "*Geometrization of Physics III*", *Kazan State Univ., Kazan, 1 – 5 October 1997*, p. 153
156. Bashkov V I, Sintsova Yu V *Gravitation Cosmology* **5** 319 (1999)
157. Bashkov V I, Sintsova Yu V *Rep. Math. Phys.* **48** 353 (2001)
158. Bashkov V I, Staroverova M E *Izv. Vyssh. Uchebn. Zaved. Fiz.* **45** (6) 95 (2002) [*Russ. Phys. J.* **45** 645 (2002)]
159. Kocharovskiĭ Vl V "Linear interaction between electromagnetic waves in inhomogeneous weakly anisotropic media", PhD Thesis (Gor'kiĭ: IPF RAN, 1985) p. 42
160. Rivlin L A *Quantum Semiclas. Opt.* **10** 299 (1998)